RICE UNIVERSITY
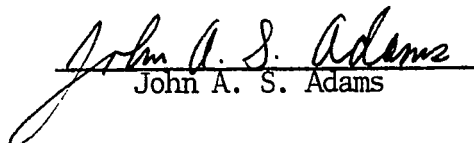

Application of the Potassium-Argon Method

to the

Dating of Shocked Rocks

by
Jack B. Hartung

A THESIS SUBMITTED
IN PARTIAL FULFILLMENT OF THE
REQUIREMENTS FOR THE DEGREE OF

DOCTOR OF PHILOSOPHY

Thesis Director's Signature

John A. S. Adams

Houston, Texas

May, 1968

TABLE OF CONTENTS

LIST OF TABLES AND FIGURES

i

INTRODUCTION

K-Ar analysis is usually applied to igneous rocks to determine the time the rock crystallized from a liquid phase and began to retain radiogenic argon. A strong shock event might render a rock or particular mineral phase incapable of complete radiogenic argon retention. The ordinary K-Ar age determined for such a shocked rock would be invalid. This problem may be especially serious for samples from the lunar surface, which is believed by many students of the moon to have been subjected to numerous impact shock events. The first objective of the present study was to determine the characteristics related to a shock event required to render a rock incapable of complete argon retention.

To determine the time of a shock event using K-Ar analysis requires first that complete radiogenic argon release occurs as a result of the shock event. The second objective of this study was to determine the characteristics related to a shock event required to produce complete radiogenic argon release from a rock.

Determining the time of the shock event also required complete radiogenic argon retention after the shock event. The final objective of the study was to establish criteria for selecting samples for which a reliable age for the shock event may be obtained.

The first set of samples used in this study were shocked by nuclear test explosions at the Nevada test site. The second set of samples were shocked by the meteorite impact event forming the Brent crater in Ontario, Canada.

HARDHAT-SEDAN SAMPLES

Four samples shocked by nuclear explosion were taken from cores drilled after the 5-kiloton Hardhat nuclear test event which was wholly contained underground. Petrographic data and other information related to this event and these samples have been described by Short (1966). Three samples were taken from the ejecta from the 100-kiloton Sedan crater-forming nuclear test event. All three of the samples were shock metamorphosed to a greater extent than the most highly shocked Hardhat sample. In addition, because the Sedan samples were thrown into the air and landed on the ground, they cooled much more quickly than the Hardhat samples. The three remaining samples analyzed were preshot or unshocked. All the samples were originally part of the Climax grano-diorite stock, which is located on the Nevada Test Site (Houser and Poole, 1959).

Included in Table I are the peak shock pressures experienced by the samples. Peak shock pressures for the Hardhat samples were calculated by Butkovich (1965) as a function of the preshot sample distance from the detonation point. The peak shock pressures for the Sedan samples have been qualitatively estimated by Short (1967) based on a petrographic comparison between the Hardhat and Sedan samples.

For each sample biotite and feldspar plus quartz mineral separates were obtained by the author. Potassium concentrations were determined for each mineral separate, as well as for the whole rock samples, by potassium tetraphenylboron precipitation, and by flame atomic absorption spectrophotometry. Radiogenic Ar^{40} concentrations were measured by iso-tope dilution mass spectrometry. The detailed procedures, calculations,

and error analysis for the K-Ar method are presented in Appendices I
through V.

The results of K-Ar analysis of all the samples are presented in
Table I. The age of the Climax stock, as indicated by the average of
the unshocked biotite apparent ages, is 106 million years. The combined
feldspar and quartz mineral separates tend to yield lower apparent ages.
This tendency is consistent with the conclusion recently reviewed by
Fechtig and Kalbitzer (1966) that argon is lost by diffusion through the
feldspar lattice more easily than through the biotite lattice.

Several terms require clarification at this point. A shock event
refers to an occurrence, such as a nuclear explosion or a large meteorite
impact, which produced a shock wave in the earth. From the standpoint of
a particular sample, shock effects are mechanical effects produced in the
sample by the passage of the shock front. Associated with the presence
of a shock front there is a thermal spike which instantaneously heats
the sample. With the passage of the rarefaction following the shock
front, the sample is instantaneously cooled, but only partially, thus
leaving the sample at an elevated residual temperature. Thermal effects
are produced in a sample by both the thermal spike and the residual thermal
environment. Shock metamorphism refers to the changes that occur in the
minerals and consists of both shock and thermal effects. Considered at
the level of the crystal lattice, shock and thermal processes are closely
related, since both serve to increase the kinetic energy of the individual
atoms. However, the input of shock related energy occurs rapidly along
a well defined surface which moves in a definite direction, while the
increase of thermal energy implies a homogeneous non-directional process.

Apparent ages of samples taken after the Hardhat nuclear test event
are plotted in figure 1 as a function of increasing shock metamorphism.
Biotite samples lost little or no radiogenic argon as a result of the
shock event. However, feldspar samples show definite radiogenic Ar^{40}
loss. Almost 90 percent of the radiogenic argon was lost from feldspars
from the most highly shocked Hardhat sample (28-1006). Based on the
temperature and peak shock pressure data developed by McQueen, Marsh, and
Fritz (1967) for granites, the thermal spike associated with the passage
of the whock wave of 100 to 200 kilobars peak pressure would have a
maximum temperature of less than 200°C. The residual temperature in the
rock immediately after passage of the shock wave would be less than the
maximum temperature. This aspect of the temperature environment experienced
by sample 28-1006 was considered incapable of causing the radiogenic
argon loss observed. The Hardhat samples were located so that those
experiencing the greatest shock pressures also experienced the most
prolonged heating due to the puddle of fused material produced by the
explosion. At this point it was not possible to determine whether the
radiogenic argon loss was due strictly to shock effects or to long term
thermal effects or to some combination of the two.

Argon loss as a shock effect is envisioned in the following way.
The passage of a shock front severely damages the sample, thus reducing
its effective grain size or disrupting its crystal lattice. Argon
trapped in the lattice will then have a much shorter and/or easier path
to grain boundaries. Argon loss as a thermal effect is viewed simply as
a result of an increased diffusion rate produced by the higher temperatures.

Evidence indicating major reductions in the effective grain size of
shocked rocks is abundant. Coarse grained quartz and feldspar crystals

shocked above 100 kilobars peak pressure may be reduced to a powder by crumbling the sample between the fingers. Studies correlating peak shock pressure with the extent of microfracturing in a sample have been done by Short (1966). Single crystal x-ray diffraction studies of grains of Hardhat sample 28-1006, which was shocked above 100 kilobars, give a preferred orientation pattern (Taylor, 1967). This result indicates a single grain is essentially a polycrystalline mass on the submicroscopic scale.

Considering the above, it is tempting to attribute the argon loss observed primarily to shock effects rather than thermal effects. To resolve this uncertainty, three samples shocked during the Sedan nuclear test event were analyzed for potassium and Ar^{40} by the author. All of these samples were more intensely shock metamorphosed than the Hardhat samples; hence, they might be expected to be more thoroughly depleted in argon. The most severely shock metamorphosed of these samples (Sedan-3) was largely isotropized, but not fused. No flow structure was observed, and pre-shock crystal forms were recognizable (Short, 1967).

The results of the analysis of Sedan samples are also included in figure 1.

Biotite samples still retained most of their radiogenic argon, and in this case the feldspar samples also retained most of their radiogenic argon. These results support the following conclusions:

1. Long periods of high temperatures are more important than high shock pressures in causing complete argon loss from feldspar minerals.

2. A strong shock wave (greater than 200 kilobars peak pressure) and only the temperature increase directly related to the

passage of the shock front are sufficient to cause significant (at least 40 percent) but not total argon loss from isotropized, but unfused grains.

3. Certain temperature-time profiles may exist following a shock event, such that a feldspar grain will lose nearly all its radiogenic Ar^{40} and an associated biotite grain will retain essentially all of its radiogenic Ar^{40}.

It has been shown by Fredriksson and De Carli (1964) that argon may be implanted into a crystal lattice by a shock process in the laboratory. Higher atmospheric argon components observed during this study in the more highly shocked Hardhat and Sedan samples indicate the addition of some atmosphere gas as a result of the shock event. The process involved could be either implantation of gas atoms in the crystal lattice or adsorption of gases on the surfaces of microfractures produced by the passage of the shock wave. The author favors the latter inter-pretation. A stepwise heating experiment similar to those reported upon by Kirsten and Muller (1967) could be expected to detect a component of gas shocked into the lattice of crystals.

In all cases but one, shocked feldspar grains lost more radiogenic argon than shocked biotite grains. The most highly shocked sample (Sedan-3), which was extensively isotropized, produced the one anomalous result. The difference is greater than the errors involved, but the anomaly could have been due to inhomogeneous samples produced by poor mineral separations, which were characteristic of the more highly shocked samples. If the anomaly is real, that is if the biotite phase lost more radiogenic argon than the feldspar phase for this sample, an hypothesis explaining it must involve for highly shock metamorphosed samples either

a tightening of the feldspar phase with respect to argon loss or a sharp decrease in the ability of the biotite phase to hold argon.

TABLE I.   RESULTS OF K-Ar ANALYSIS OF HARDHAT AND SEDAN SAMPLES

Peak Shock Pressure,[1] Kilobars	Sample Number	Type	K Conc., Percent	Radiogenic Ar^{40} Percent[2]	Rad. Ar^{40} Conc., (moles/gm) x 10^9	Apparent Age, m.y.	Probable Error, m.y.
0	Unshocked Surface	W.R.[3]	2.49	67.	0.456	100.	6.
		F.-Q.[4]	1.95	64.	0.378	106.	7.
		Bio.[5]	6.75	76.	1.235	100.	5.
0	Preshot 191	W.R.	2.83	76.	0.522	101.	6.
		F.-Q.	2.66	79.	0.473	98.	6.
		Bio.	5.40	67.	1.113	112.	6.
0	Preshot 226	W.R.	2.80	83.	0.520	102.	6.
		F.-Q	2.41	77.	0.457	104.	6.
		Bio.	6.02	72.	1.165	106.	5.
13.	B-60	W.R.	3.24	71.	0.613	104.	6.
		F.-Q.	3.59	78.	0.650	99.	5.
		Bio.	2.57	61.	0.569	121.	8.
60.	H-108	W.R.	2.58	78	0.498	106.	6.
		F.-Q.	2.45	71.	0.461	103.	6.
		Bio.	5.23	38.	1.113	116.	8.

TABLE I (CONTINUED). RESULTS OF K-Ar ANALYSIS OF HARDHAT AND SEDAN SAMPLES

Peak Shock Pressure, Kilobars	Sample Number	Type	K Conc., Percent	Radiogenic Ar^{40} Percent	Rad. Ar^{40} Conc., (moles/gm) x 10^9	Apparent Age, m.y.	Probable Error, m.y.
75.	28-995	W.R.	2.40	71.	0.306	71.	4.
		F.-Q.	1.90	65.	0.211	66.	5.
		Bio.	5.14	66.	1.057	112.	6.
110.	28-1006	W.R.	2.32	28.	0.136	33.	3.
		F.-Q.	2.01	22.	0.044	12.	1.
		Bio.	6.29	64.	1.141	99.	5.
150.- 250.	Sedan-1	W.R.	2.83	81.	0.486	94.	5.
		F.-Q	2.78	68.	0.508	100.	6.
		Bio.	4.70	49.	0.940	109	6.
200. - 300.	Sedan - 2	W.R.	2.44	54.	0.413	93.	6.
		F.-Q.	1.89	47.	0.282	82.	6.
		Bio.	4.99	62.	0.941	103.	6.
300. - 400.	Sedan - 3	W.R.	3.72	51.	0.507	75.	5.
		F.-Q.	3.54	52.	0.478	75.	5.
		Bio.	4.63	35.	0.502	59.	4.

TABLE I (CONTINUED). RESULTS OF K-Ar ANALYSIS OF HARDHAT AND SEDAN SAMPLES

Footnotes:

1. Peak shock pressure from Short (1966) and Short (1967).

2. Radiogenic Ar^{40}, percent $= \dfrac{Ar^{40} \text{ (radiogenic)}}{Ar^{40} \text{ (radiogenic)} + Ar^{40} \text{ (atmospheric)}} \times 100$

3. W.R. = Whole Rock

4. F.-Q. = Feldspar + Quartz
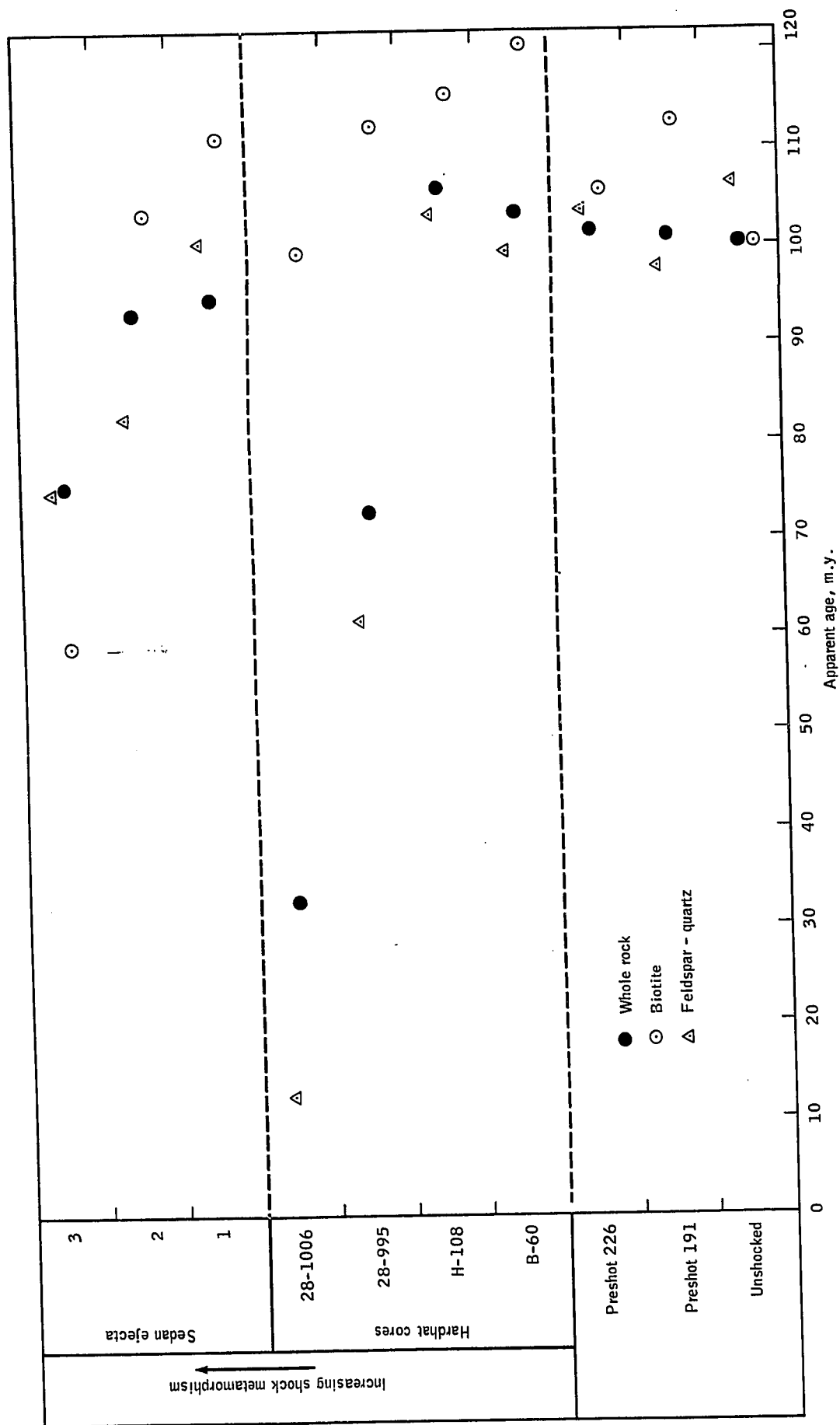
5. Bio. = Biotite

Figure 1. - Results of K-Ar analysis of hardhat and sedan samples.

BRENT CRATER SAMPLES

The results of geological and geophysical work on the Brent Crater have been reported by Millman, et al. (1960). More recently, Dence (1968) has made a detailed petrographic study of samples from drill cores which penetrate the Brent crater at various locations. This paper reports on the results of K-Ar dating of samples taken from a single drill core (B1-59) which penetrates the center of the Brent Crater. Dence (1968) has used this same core as a type section in the development of a sequence of shock metamorphic grades. In addition, three samples collected from the ground surface outside the area of the crater were analyzed. The sample preparation, potassium concentration determination, and radiogenic Ar^{40} concentration determination procedures are described in detail in Appendices I, II, and III, respectively.

The data obtained from K-Ar analysis of the Brent samples are presented in Table II.

According to Dence (1968), the relatively undisturbed country rocks underlying the crater are gneisses of granodioritic composition with rare bands of amphibolite and gabbro. The primary minerals are quartz, alkali feldspar, plagioclase near An_{30}, amphibole, and biotite. Garnet, iron ore, and apatite are accessory minerals. The alkali feldspar is commonly a microcline mesoperthite. Pegmatitic rocks containing quartz, alkali feldspar, oligoclase, and mica also occur.

The K-Ar age of the country rock in the vicinity of the Brent Crater may not be stated definitely based only on the data obtained by the author. However, the crater is located in the Grenville province of the Canadian shield, which has been shown to have a K-Ar age of 900-950 m.y. (Wetherill, 1966).

The apparent ages determined for samples from the drill core (B1-59) are plotted against depth of the sample below the present land surface in figure 2. The location of original crater features is indicated in figure 3, a schematic drawing of the crater from Dence (1968).

The deepest samples analyzed were the least affected by the crater-forming event. Whole rock analyses of these samples yield ages of 800 m.y. or less. These low ages for Grenville province rocks are due to radiogenic argon loss produced by one or more of the following factors:

1. Relatively poor argon retention capacity of the feldspar lattice.

2. Increased diffusion rate of argon due to a higher temperature produced by the crater-forming event.

3. Increased diffusion rate of argon due to a higher temperature existing at the sample depth.

4. Argon loss associated with the forming of perthitic exsolution bands, which are abundant in the samples analyzed (Fechtig and Kalbitzer, 1966).

The predominantly hornblende mineral separates for the deepest sample, 3463, and for one of the samples collected from the ground surface, Brent Surface-2, yield ages of 1480. $\pm$ 80 m.y. and 1570. $\pm$ 80 m.y., respectively. These high ages are due either to excess Ar^{40} trapped in the hornblende lattice at the time of crystallization or to relict grains of hornblende which retained Ar^{40} throughout the metamorphism which produced the Grenville rocks. Pearson, et al. (1966), have reported a similar inconsistency based on an analysis of one hornblende sample. Damon (1967) considers such an inconsistency due to excess argon as opposed to relict grains. Petrographic study by the author does not support the view that the grains are relict, but Tilton and Hart (1963)

and Hanson and Gast (1967) have shown hornblende to be significantly more retentive with respect to Ar^{40} than biotite or feldspar. Neither the literature nor the data produced by our study provide an adequate explanation of the anomalously high hornblende ages. We suggest, as a possible step toward resolving this problem, that a step-wise heating experiment, similar to those reported by Kirsten and Müller (1967), be undertaken. Detection of two components of radiogenic Ar^{40} by such an experiment would indicate the presence of excess argon rather than relict grains.

Three other ferromagnesian mineral separates containing biotite and hornblende, samples 3112, 3018.3, and Brent Surface-1, give normal Grenville ages, 910. ± 40. m.y., 890. ± 50. m.y., and 890. ± 40. m.y., respectively. Two additional samples, 2938. and Brent Surface-3, produced ages between 900. m.y. and 1500. m.y. These results indicate to the author that there are two types of ferromagnesian minerals in the essentially unshocked samples. One type yields an age of 1500. m.y., the other a normal age of 900 m.y. In addition, some samples contain a mixture of the two. Hornblende is the mineral responsible for the anomalously high apparent ages, but there is no direct relationship between mineralogy and apparent age, since hornblende is abundant in samples giving the lower ages as well.

As one proceeds up the core to a depth of 2880 feet below the surface, the samples are increasingly shock metamorphosed, but their original texture and mineralogy are still recognizable, although some recrystallization of quartz is observed. Hornblende is partially replaced by biotite, a change which existed in the rocks before the crater-forming event. Additional petrographic data have been presented in detail by Dence (1968).

The apparent ages determined for both feldspar and ferromagnesian mineral separates decrease to a value of about 400 m.y. This decline is interpreted by the author as a result of higher rates of diffusion in those rocks subjected to the higher temperatures near the melted "puddle." The ferromagnesian mineral separates for each of these samples yield a 100 to 200 m.y. higher apparent age than each respective feldspar plus quartz mineral separate. This reconfirms the view that hornblende and biotite lattices are tighter with respect to the loss of radiogenic Ar^{40} than potassium feldspar.

The Samples immediately beneath the "puddle," between 2880 feet and 2800 feet below the surface, are a mixture of highly shocked and altered rocks and completely recrystallized rocks. Mineral separates obtained for these samples were of poor quality. All separates analyzed gave ages that are considered by the author to be anomalously low. The ages below 400 m.y. for the highly shocked, but unrecrystallized, samples are interpreted by the author to be due to a higher argon diffusion rate in the lattices damaged by the shock wave.

The "puddle" referred to above is about 100 feet thick and consists of crystals formed after the shock event. The crystals are not deformed and show no evidence of shock metamorphism. Samples containing only new crystals are identified by an asterisk in Table II. The boundaries between the "puddle" and the highly shock metamorphosed country rock are not well defined. Judging from the one drill core penetrating the "puddle," cracks filled with "puddle" material radiate into the country rock, or blocks of country rock occur inside the "puddle."

Samples composed of entirely new crystals are of two types. Those located near the boundaries of the "puddle" are fine grained (less than

0.5 mm in diameter) and consist of radiating crystals of potassium feld-
spar and interstitial chlorite. These samples yield apparent ages of less
than 400 m.y. Such low ages are interpreted by the author to represent
delayed closure of the system due to devitrification of a glass produced
at the time of the Brent event. The sample located near the center of
the "puddle" (sample 2771.4) consists of well-formed potassium feldspar
and chlorite with grain sizes from 1 to 2 mm across. The texture and
crystal morphology displayed by this sample is interpreted by the author
to indicate that the sample crystallized from a melt. A whole rock
apparent age of 426. ± 20. m.y. was obtained for this sample. Since this
is the oldest age for a sample with new crystals, and since the sample
crystallized from a melt, this age represents the best estimate for the
minimum age of the crater-forming event. Considering the errors in the
K-Ar method, the possible extent of argon loss since crystallization,
and the uncertainties in the stratigraphic time scale, this age may be
considered consistent with the presence of middle Ordovician (450-470 m.y.)
sediments reported by Millman, Liberty, et al. (1960), inside the crater
itself.

It was indicated above that petrographic and radiometric age differ-
ences allow a distinction to be made between new crystals formed by
devitrification and by crystallization from a melt. In addition, it was
observed by the author that those samples which existed for some time as
a glass also have anomalously high potassium concentrations. This
correlation is interpreted by the author as due to a post-event potassium-
rich hydrothermal alteration which affected the glasses surrounding the
melted "puddle," but did not affect the melted material of the "puddle."
The source of energy for the hydrothermal activity is believed by Mr. M. R.

Dence and the author to be impact event itself, since no evidence for hydrothermal activity has been found in the area around the crater.

One sample of breccia, produced by the fallback of debris into the crater, was analyzed. The feldspar plus quartz separate gave an age of 416. ± 18. m.y., and the ferromagnesian separate gave an age of 440. ± 20. m.y. These results suggest rather complete radiogenic Ar^{40} loss at the time of the crater-forming event. The pre-event texture and mineralogy are easily recognizable in the sample. According to Dence (1967), the sample was shock metamorphosed to an extent similar to the samples between 2900 and 2920 feet. The sample was located at 1305 feet below the surface or over 1400 feet above the "puddle" and about 500 feet below the fresh crater floor. It represents a naturally shocked example corresponding to the Sedan ejecta samples discussed in the previous section. The Sedan samples were highly shock metamorphosed, but cooled rapidly and retained most of their radiogenic Ar^{40}. The Brent sample was shock metamorphosed, but not so strongly, and apparently lost essentially all of its radiogenic Ar^{40} at the time of the crater-forming event. Apparently some mechanism existed under the Brent crater to maintain temperatures high enough for radiogenic Ar^{40} to diffuse out of the grains. Based on the results for the Sedan ejecta samples reported in the previous section, the temperatures associated with the passage of the shock front are not sufficient to produce argon loss. Neither the residual temperature decay in the material surrounding the sample nor conduction of heat from the fused "puddle" is believed to be sufficient to produce the observed argon loss. The alternative method suggested for heating the breccia sample is by convection of super heated fluids produced near the "puddle". The anomalously high potassium concentration in this sample also indicates it was subjected to a period of hydrothermal alteration.

A summary of the author's interpretations of the results obtained for the Brent crater samples is presented in figure 4. A plot similar to figure 2 is presented with only the whole rock K-Ar ages indicated. Curves are drawn to indicate the trends inferred from the data. The following types of samples are indicated on the figure.

1. Unaffected country rock beneath the crater.

2. Samples partially depleted in radiogenic Ar^{40} during Brent event.

3. Samples totally depleted in radiogenic Ar^{40} during Brent event and rendered incapable of total Ar^{40} retention following the event.

4. Samples with new crystals formed by devitrification of glass formed at the edges of the "puddle."

5. Samples with new crystals formed by crystallization from the melt at the interior of the "puddle."

Additional types of samples analyzed but not indicated on figure 4 are:

1. One sample of allochtonous breccia depleted in Ar^{40} during the Brent event.

2. Samples of surface rocks surrounding the crater.

The following conclusions are supported by the results from the Brent crater samples:

1. Significant radiogenic argon loss was detected only in rocks showing definite evidence of at least moderate shock metamorphism (grade iv of Dence, 1968) and hydrothermal alteration or recrystallization.

2. Samples which have been strongly shock metamorphosed (grade vi of Dence, 1968) and hydrothermally altered or partially or poorly recrystallized may lose essentially all of their radiogenic argon in the process, but they also lose their capacity for complete argon retention following the shock event.

3. New crystals formed by devitrification may be distinguished from those crystallized from a melt based on their petrographic appearance and K-Ar age.

4. Only samples crystallized from a melt are considered reliable from the standpoint of obtaining an accurate date for an event.

5. The Brent meteorite impact occurred a minimum of 426. $\pm$ 20. million years ago.

6. A period of potassium-rich hydrothermal activity was generated by the Brent event.

TABLE II. RESULTS OF K-Ar ANALYSIS OF BRENT CRATER SAMPLES

Sample No.	Type	K Conc., Percent	Radiogenic Ar^{40}, Percent	Rad. Ar^{40} Conc., (moles/gm) x 10^9	Apparent Age, m.y.	Probable Error, m.y.
3463	W.R.[2]	4.49	95.	7.99	800.	30.
	F.-Q.[3]	5.08	97.	8.12	740.	30.
	Ferro.[4]	1.64	97.	6.52	1480.	80.
3112	W.R.	4.14	96.	7.18	790.	30.
	Ferro	1.44	90.	2.98	910.	50.
3018.3	W.R.	4.03	96.	6.75	770.	30.
	Ferro	1.34	94.	2.72	890.	50.
2962	W.R.	4.04	94.	6.56	740.	30.
	Ferro	0.74	81.	1.11	700.	60.
2938	W.R.	4.16	94.	7.05	770.	30.
	F.-Q.	7.96	98.	12.89	740.	30.
	Ferro	0.87	79.	2.74	1250.	110.

TABLE II.   RESULTS OF K-Ar ANALYSIS OF BRENT CRATER SAMPLES

Sample No.	Type	K Conc., Percent	Radiogenic Ar^{40}, Percent	Rad. Ar^{40} Conc., (moles/gm) x 10^9	Apparent Age, m.y.	Probable Error, m.y.
2916.6	W.R.	3.46	85.	3.27	470.	20.
	F.-Q.	4.26	87.	4.80	550.	20.
	Ferro	1.64	84	2.23	640.	40.
2900	W.R.	3.81	72.	3.35	440.	20.
	F.-Q.	6.69	80.	4.85	368.	17.
	Ferro	1.31	77.	1.59	580.	40.
2888	W.R.	5.73	89.	4.29	380.	17.
	F.-Q.	6.67	84.	5.00	380.	17.
	Ferro	2.27	83.	2.24	490.	30.
2870	W.R.	5.61	89.	4.16	377.	17.
	Ferro	1.92	88.	1.56	410.	30.
2842 *	W.R.	8.55	92.	5.60	336.	15.
	Ferro	5.20	90.	3.69	362.	16.
2827.5	W.R.	5.67	92.	4.33	386.	17.

TABLE II. RESULTS OF K-Ar ANALYSIS OF BRENT CRATER SAMPLES

Sample No.	Type	K Conc., Percent	Radiogenic Ar^{40}, Percent	Rad. Ar^{40} Conc., (moles/gm) $\times 10^9$	Apparent Age, m.y.	Probable Error, m.y.
2813 *	W.R.	8.05	89.	5.01	321.	14.
	F.-Q.	8.18	88.	4.75	301.	13.
	Ferro	5.97	91.	3.92	337.	15.
2800 *	W.R.	5.14	82.	3.56	354.	16.
2771.4 *	W.R.	4.26	93.	3.62	426.	20.
2757 *	W.R.	6.19	85.	4.10	339.	15.
2723 *	W.R.	6.12	62.	4.06	340.	16.
1305 **	W.R.	6.57	91.	5.25	403.	18.
	F.-Q.	10.43	91.	8.63	416.	18.
	Ferro	2.71	87.	2.38	440.	20.
Brent Surface-1	Ferro	3.99	94.	8.11	890.	40.
Brent Surface-2	Ferro	1.34	94.	5.84	1570.	80.
Brent Surface-3	Ferro	1.75	92.	5.03	1170.	60.

23

TABLE II. RESULTS OF K-Ar ANALYSIS OF BRENT CRATER SAMPLES

* Sample contains only new crystals

** Sample of allochtonous breccia

1. Radiogenic Ar^{40}, percent $= \dfrac{Ar^{40}(\text{radiogenic})}{Ar^{40}(\text{radiogenic}) + Ar^{40}(\text{atmospheric})}$

2. W.R. = Whole Rock
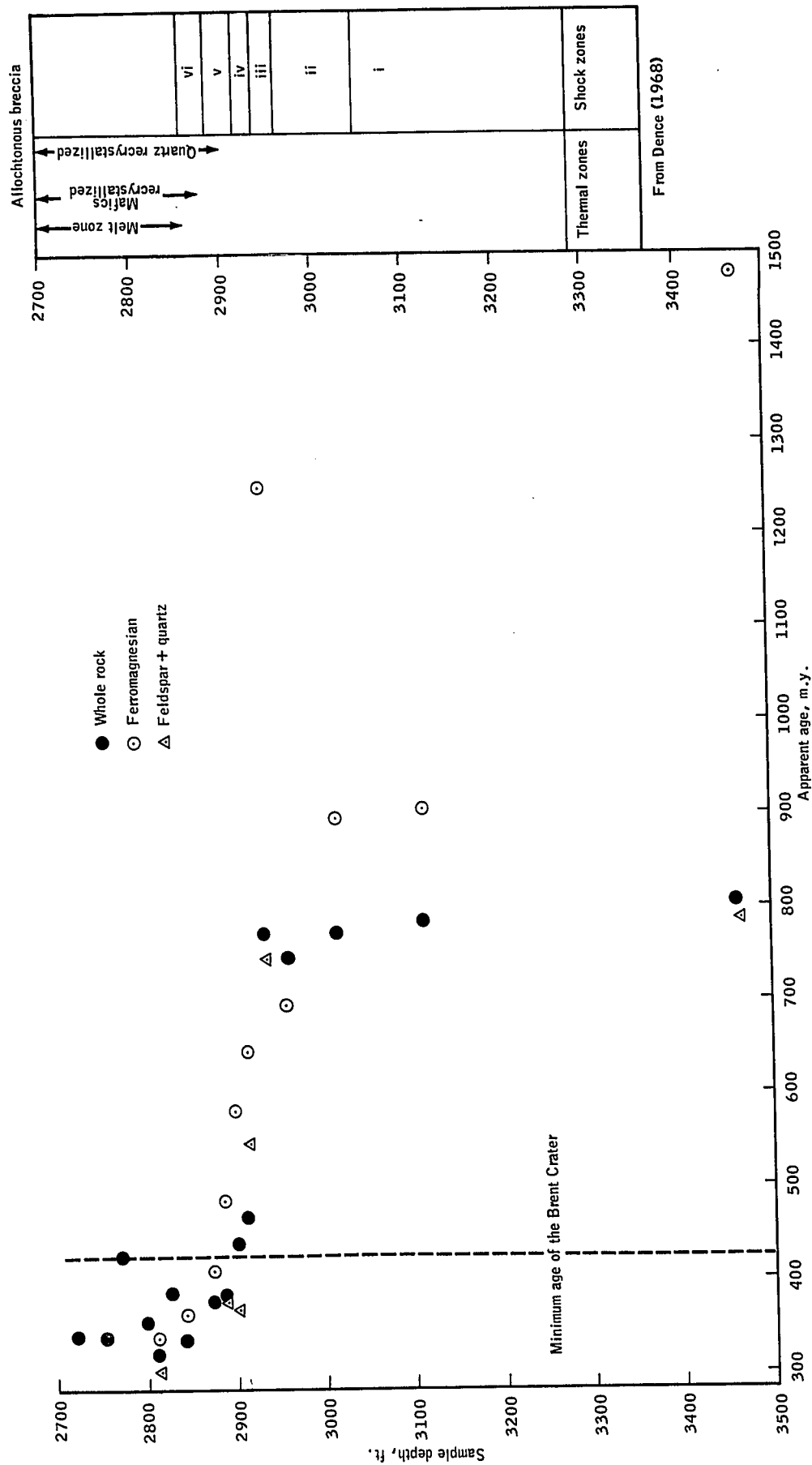
3. F.-Q. = Feldspar + Quartz

4. Ferro = Ferromagnesian

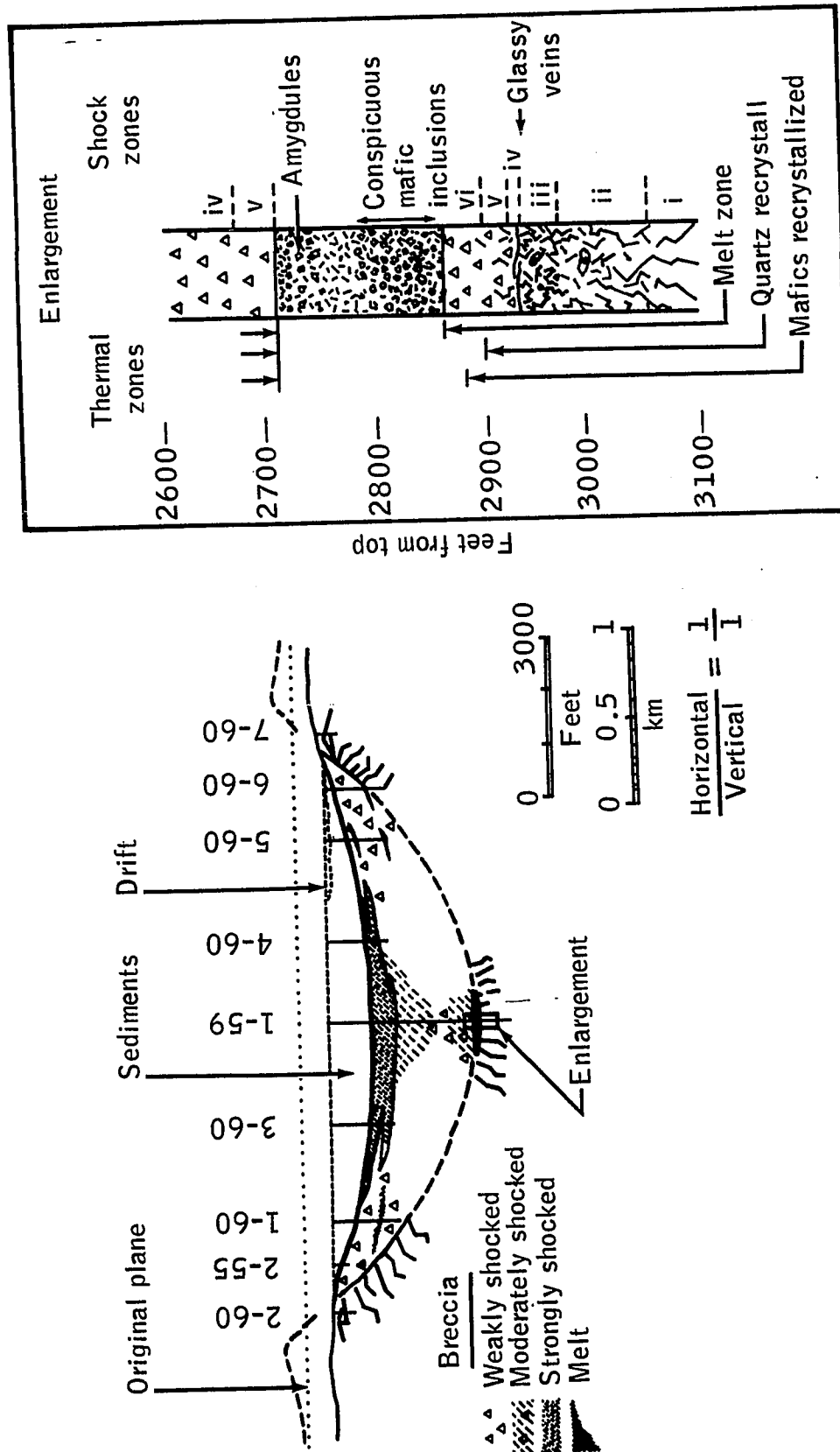Figure 2. – Results of K-Ar analysis of Brent Crater samples.

Figure 3. - Location of Brent Crater features from Dence (1968).

Allochtonous breccia

Melt zone

Mafics recrystallized

Quartz recrystallized

vi
v
iv
iii

ii

i

Thermal zones | Shock zones

From Dence (1968)

2700
2800
2900
3000
3100
3200
3300
3400

1500 1400 1300 1200 1100 1000 900 800 700 600 500 400 300

Apparent age, m.y.

Sample depth, ft.

2700
2800
2900
3000
3100
3200
3300
3400
3500

Type 1.

Type 2.

Type 3.

Type 4.

Type 5.

Type 1. Unaffected
2. Partial loss of Ar^{40}
3. Total loss of Ar^{40}
4. New crystals formed by devitrification
5. New crystals formed by crystallization from a melt

● Data for whole rock samples

—— Pre-Brent crystals present

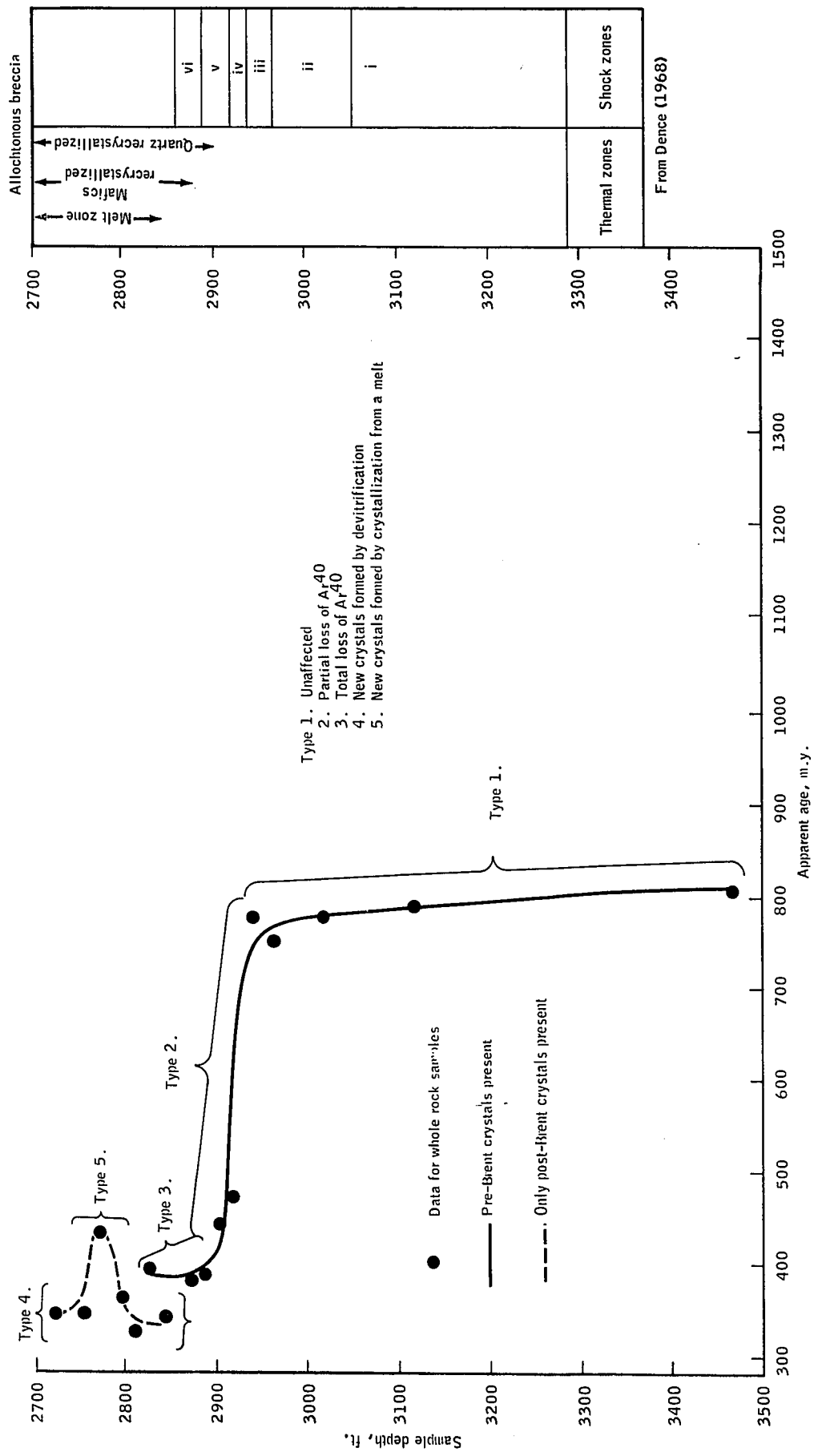----- Only post-Brent crystals present

Figure 4. - Location of the types of samples produced by the Brent impact event.

CONCLUDING REMARKS

In general, argon losses detected in unmelted samples could be attributed to diffusion rates, which increased in response to increases in the local temperature. Higher local temperatures were produced or maintained in one of the following ways:

1. Passage of a shock front.

2. Conduction of heat from a nearby source.

3. Convection of hot fluids produced nearby.

Although shock damage to crystal lattices may have been a factor in allowing higher argon diffusion rates, no direct evidence was obtained which demonstrated this factor.

Samples which crystallized relatively slowly from a melt are the only reliable indicators of the age of the event which produced the melt. Accurate absolute K-Ar dating of small lunar craters, those in which no melt zone was produced, will not be possible. K-Ar dating of larger craters will require samples of material melted by the crater-forming event. However, it should be noted that other dating methods, such as the cosmic ray exposure time, may be used to determine the age of a lunar crater using samples from the surface.

Samples collected for the purpose of K-Ar dating the host rock near an impact crater may show signs of mild shock metamorphism (grade ii of Dence, 1968) and still be expected to yield a reliable age. When collecting samples for the purpose of K-Ar dating a shock event, every effort should be made to obtain material which crystallized from a melt produced by the shock event. If this is not possible, homogeneous glasses produced by the shock event may be used, but with somewhat less confidence in the K-Ar age obtained.

The study described in the preceding pages consisted essentially of gathering rather detailed K-Ar data related to essentially uncontrolled shock events. The results obtained serve primarily to confirm already existing ideas about the response of radiogenic argon in a crystal lattice to a shock event. Based on the results obtained here, further studies are indicated in the following areas:

1. Develop a pressure-temperature-time history model associated with the Brent impact event.

2. Selectively sample and date other impact structures in order to test the conclusions developed here and the model of environmental conditions related to shock event indicated above.

3. Study the ejecta material produced by a shock cratering event in an attempt to correlate argon loss with the position of the ejecta material.

4. Perform step-wise heating experiments with the hornblendes from samples giving anomalously high ages to determine the source of the excess argon observed.

5. Execute controlled laboratory experiments with varying shock pressure-temperature-time environments in an effort to simulate and understand more completely the processes that occurred under natural conditions.

ACKNOWLEDGEMENTS

REFERENCES

Aldrich, L. T., and Wetherill, G. W., 1958
　　Ann. Rev. of Nucl. Sci., vol. 8, p. 257
　　Geochronology by radioactive decay

Belcher, R., and Wilson, C. L., 1955
　　New Methods in Analytical Chemistry
　　Chapman and Hall, London

Butkovich, T. R., 1965
　　Jour. of Geophysical Res., vol. 70, p. 885
　　Calculation of the shock wave from an underground nuclear explosion
　　　in granite

Damon, P. E., Laughlin, A. W., and Percious, J. K., 1967
　　in Proceedings of the symposium, Radioactive Dating and Methods of
　　　Low-Level Counting
　　Problem of excess argon-40 in volcanic rocks
　　International Atomic Energy Agency, Vienna

Dean, J. A., 1960
　　Flame Photometry
　　McGraw-Hill Book Co., New York

Dence, M. R., 1967
　　Private Communication
　　Shock metamorphic grade of allochtonous breccia sample

Dence, M. R., 1968
　　in Shock Metamorphism of Natural Materials edited by B. French and
　　　N. M. Short
　　Shock zoning at Canadian craters:　petrography and structural
　　　implications
　　Mono Press Corp., Baltimore

Fechtig, H., and Kalbitzer, S., 1966
　　in Potassium Argon Dating, compiled by O. A. Schaeffer and
　　　J. Zahringer
　　The diffusion of argon in potassium-bearing solids
　　Springer-Verlag New York, Inc.

Fredriksson, K., and De Carli, P., 1964
　　Jour. of Geophysical Res., vol. 69, no. 7, p. 1403
　　Shock emplaced argon in a stony meteorite

Hanson, G. N., Gast, P. W., 1967
　　Geoch. et Cosmoch. Acta, vol. 31, no. 7, p. 1119
　　Kinetic studies in contact metamorphic zones

Hintenberger, H., 1949
　　Rev. Sci. Inst., vol. 20, no. 10, p. 748
　　Improved magnetic focusing of charged particles

Houser, F. N., and Poole, F. G., 1959
    U.S. Geol. Survey Report TEM 836A
    Granite exploration hole, Area 15, Nevada Test Site, Nye County,
        Nevada

Houtermans, F. G., 1966
    in Potassium Argon Dating, compiled by O. A. Schaeffer and
        J. Zahringer
    History of the K-Ar method of geochronology
    Springer-Verlag New York, Inc.

Kerwin, L., 1949
    Rev. Sci. Inst., vol. 20, no. 1, p. 36
    Improved magnetic focusing of charged particles

Kirsten, T., and Muller, O., 1967
    in Proceedings of the symposium, Radioactive Dating and Methods of
        Low-Level Counting
    Argon and potassium in mineral fractions of three ultramafic rocks
        from the Baltic shield
    International Atomic Energy Agency, Vienna

Lanphere, M. A., and Dalrymple, G. B., 1967
    Geoch. et Cosmoch. Acta, vol. 31, p. 1091
    K-Ar and Rb-Sr measurements on P-207, the U.S.G.S. interlaboratory
        standard muscovite

Letolle, R., 1966
    Geol. Rundschau, vol. 55(1), p. 197
    Natural isotopic variation of potassium: results, perspectives,
        and interpretations

Lipson, Joseph, 1958
    Bull. of the Geol. Soc. of Am., vol. 69, p. 137
    Potassium-argon dating of sedimentary rocks

McQueen, R. G., Marsh, S. P., and Fritz, J. H., 1967
    Jour. of Geophysical Res., vol. 72, no. 20, p. 4999
    Hugoniot equation of state of twelve rocks

Millman, P. M., Liberty, B. A., Clark, J. F., Willmore, P. L., and
        Innes, M. J. S., 1960
    Publication of the Dominion Observatory, vol. 24(1)
    The Brent Crater

Nier, A. O., 1947
    Rev. Sci. Inst., vol. 18, no. 6, p. 398
    A mass spectrometer for isotope and gas analysis

Nier, A. O., 1950
    Phys. Rev., vol. 77, pp. 789-793
    Determination of the relative abundances of the isotopes of carbon,
        nitrogen, oxygen, argon, and potassium

Pearson, R. C., Hedge, C. E., Thomas, H. H., Stern, T. W., 1966
     Bull. of the Geol. Soc. of Am., vol. 77, p. 1109
     Geochronology of the St. Kevin granite and neighboring Precambrian
          rocks, northern Sawatch Range, Colorado

Scarborough, James B., 1962
     Numerical Mathematical Analysis - fifth edition
     The Johns Hopkins Press, Baltimore

Short, N. M., 1966
     Jour. of Geophysical Res., vol. 71, no. 4, p. 1195
     Effects of shock pressures from a nuclear explosion on mechanical
          and optical properties of granodiorite

Short, N. M., 1967
     Private Communication
     Estimates of peak shock pressures for Sedan samples

Taylor, G. J., 1967
     Private Communication
     Results of single crystal x-ray diffraction studies of shocked rocks

Tilton, G. R., and Hart, S. R., 1963
     Science, vol. 140, no. 3565, p. 357
     Geochronology

Wetherill, G. W., 1966
     in Potassium Argon Dating, compiled by O. A. Schaeffer and
          J. Zahringer
     K-Ar dating of Precambrian rocks
     Springer-Verlag New York, Inc.

APPENDIX I - SAMPLE PREPARATION

Since most of the samples analyzed were taken from drill cores from rocks which had experienced large changes of conditions over short distances, the amount of material available for each analysis was limited.

Each sample was ground by hand using a wrought iron mortar and pestle. Several times during the grinding of each sample, the material was sieved to recover as much of the appropriate size fraction as possible. The acceptably sized grain was required to pass through a nylon screen with holes 0.50 mm square and to be held by a similar screen with holes 0.25 mm square. In terms of mesh numbers, the portion saved for analysis was approximately the plus 48-minus 74 fraction.

Dust remaining with the sample was removed by repeated rinsing with acetone. The samples were dried and stored in glass bottles.

Mineral separations were accomplished using heavy liquid or magnetic separation techniques. The limited quantity of each sample reduced the effectiveness of mineral separation. Tetrabromoethane diluted with acetone as necessary, to reduce the density of the liquid, was used primarily to separate biotite from quartz and feldspar. The Franz isodynamic magnetic separator was used to remove highly magnetic material and to separate ferromagnesian and feldspar plus quartz fractions of a particular sample.

No chlorinated hydrocarbons or hydrochloric acid should be in or added to the samples because of the danger of forming H^1Cl^{37} ions that are indistinguishable from the ions of the Ar^{38} isotopic spike.

There is some circumstantial evidence that freshly ground and analyzed samples have less atmospheric argon correction. No pre-heating or hydrofluoric acid etch was used on these samples.

APPENDIX II - POTASSIUM CONCENTRATION DETERMINATION

Total K concentration was determined for each sample using both potassium tetraphenylboron precipitation and atomic absorption flame photometry.

Opening. Each sample was opened once using the following HF - HNO_3 treatment.

- 0.2 gm to 0.6 gm of sample was weighed into a 50 ml or 100 ml teflon beaker.

- 10 ml of HNO_3 (concentrated) was added to the beaker, which was then heated under lamps for 1 1/2 to 2 hours with teflon watchglass covers over the beakers.

- 6 ml to 10 ml of HF (concentrated) was added to the beaker which was uncovered and heated under lamps until the solution evaporated to dryness. Care was taken to avoid burning the sample as a result of heating past the point of dryness. (In some cases the HF was added before the initial heating in the first step.)

- 5 ml to 10 ml HNO_3 (concentrated) and 2 ml to 10 ml HF (concentrated) were added to the dried sample, which was again heated to dryness in the uncovered beakers. Care was taken to avoid burning the samples.

- 2 ml to 4 ml of HNO_3 (concentrated) and 40 ml to 90 ml doubly distilled H_2O was added to the dried sample. The covered beakers were heated overnight on a steam table or partially under lamps.

- a few grains of residue in the beaker were ignored, and the
sample was diluted to exactly 100.0 ml and stored in a poly-
ethylene bottle.

This solution was designated the stock solution, and was used for
both gravimetric and atomic absorption K concentration determinations.

Gravimetric Analysis. Each sample was analyzed for total K concen-
tration once using the potassium tetraphenylboron [$KB(C_6H_5)_4$] precipi-
tation method (Belcher and Wilson, 1955). A description of the procedures
used follows.

- Weigh clean filter crucible to nearest 0.0001 gm.

- Pipette 25.00 ml of stock solution into 100 ml to 250 ml
beaker.

- Add about 25 ml of H_2O

- While stirring continuously, add drop-wise 40 ml of 0.6 per-
cent sodium tetraphenylboron [$NaB(C_6H_5)_4$] reagent solution.
(Reagent solution is prepared by dissolving 1.5 gm $NaB(C_6H_5)_4$
in 250 ml of distilled H_2O.

- Allow precipitate to settle for about 10 minutes.

- Filter solution through fine porosity filter crucible of
known weight.

- Wash beaker with H_2O to assure that all the precipitate is
transferred to the filter crucible.

- Wash precipitate with potassium tetraphenylboron wash solution.
(wash solution is prepared by shaking 0.03 gm $KB(C_6H_5)_4$ in
250 ml H_2O for half an hour and filtering to remove excess
$KB(C_6H_5)_4$.)

- Dry filter crucible in oven at 105°C to 110°C for half an hour.

- Cool filter crucible in a desicator for more than two hours.

- Weigh filter crucible to nearest 0.0001 gm.

- Clean filter crucible with acetone first, then H_2O.

- Dry and cool clean filter crucible as indicated above.

- Weigh clean filter crucible to nearest 0.0001 gm.

- Store clean filter crucible in a desicator.

Total K concentration is determined using the following known or measured quantities and relationships.

Data Required:

1. Sample weight, gm

2. Stock solution initial volume, ml (usually 100 ml).

3. $KB(C_6H_5)_4$ formula weight = 358.339

4. K atomic weight = 39.102

5. Clean filter crucible weight, gm. (Usually the average of the clean filter crucible weights measured before and after a precipitation.)

6. Filter crucible plus precipitate weight, gm.

7. Stock solution analysis volume, ml (usually 25 ml).

Calculations Required:

1. Dilution factor $= \dfrac{\text{Stock solution initial volume, ml}}{\text{Sample weight, gm.}}$

2. Precipitate weight = (filter cruc. plus prec. wt, gm) - (clean filter cruc. wt, gm)

3. K weight $= \dfrac{\text{K atomic wt}}{KB(C_6H_5)_4 \text{ formula wt.}}$ x (Precipitate wt.)

4. K fraction = $\dfrac{\text{(K wt.) (Dilution factor)}}{\text{Stock solution analysis volume, ml}}$

5. %K = (K Fraction) (100)

Analysis by atomic absorption flame photometry. Each sample was analyzed once for total K concentration using atomic absorption flame photometry (Dean, 1960). An aliquot of each sample stock solution was diluted to a concentration between 0.5×10^{-6} gm/ml. This was usually accomplished by diluting 5.00 ml of the stock solution by a factor of 10 to 1 and diluting 10 ml of the resulting solution by another factor of 10 to 1.

The standard used for the atomic absorption analysis was prepared by dissolving 0.1176 gm of the Bern 4M muscovite standard and diluting the solution to a range of K concentrations from 0.5×10^{-6} gm/ml to 5×10^{-6} gm/ml. A value of 8.57 percent K was assumed for the Bern 4M muscovite standard.

Operating parameters used for the Rice University geochemistry laboratory Perkin-Elmer 214 atomic absorption spectrophotometer are as follows:

Osram lamp - potassium (allow half-hour warm up)

Lamp current - 0.65 amps

Wave length - 7554 Å (Drum setting of 2282)

Slit width - 0.5 mm

Photomultiplier power supply - 700 volts

Air pressure - 22 psi

Acetylene pressure - 10 psi

Air flow rate indicator - 5

Acetylene flow rate indicator - 4

Sensor - 1 P 28 Photomultiplier tube

Under these conditions a useful sensitivity of 0.1 x 10^{-6} gm/ml. was typical.

Using the peak heights measured for the standards of known K concentrations, a curve of peak height vs. K concentration was drawn. The sample solution peak heights were placed on the curve and their respective K concentrations were determined. The following quantities and relationships were required to produce the total K concentration.

1. Sample solution K concentration, gm/ml (measured from standard curve)

2. Sample solution dilution factor, ml/gm = (Stock solution dilution factor)(Dilution ratio)

3. K fraction, $\dfrac{gm(K)}{gm\ (sample)}$ = (Sample solution dilution factor)

4. % K = (K Fraction)(100)

K Concentration Error. Numerous sources of error exist for both gravimetric and atomic absorption K concentration determination. These errors are difficult to isolate and evaluate separately. Since two independent methods were used, an estimate of the total probable error associated with K concentration determination may be made by comparing the results of each method. A frequency distribution of the difference between atomic absorption and gravimetric K concentration determinations is presented in Appendix II figure 1.

The peak of Appendix II figure 1 occurs at 0.14%. This indicates atomic absorption results were systematically higher than gravimetric results. Since neither result is known to be correct, an average of the two results was used in subsequent calculations.

The probable error, based on the spread of the data of Appendix II figure 1, for each K concentration determination is ± 0.09%. This value may be considered the random error for K concentration determinations. It is greater than one-half the systematic difference indicated above. Thus, ± 0.1 percent was taken as the probable error for K concentration measurements. The relative probable error depends on the actual K concentration of the sample and may be expressed as follows:

$$\text{Probable error (K conc.)} = \frac{0.1\%}{\text{K conc., \%}} = \frac{\Delta \% K}{K}$$

To confirm the adequacy of the analytical techniques used, a separate rock standard, U.S.G.S. standard muscovite, P-207. was opened twice and analyzed for K concentration. Our results are compared with those reported by other laboratories (Lanphere and Dalrymple, 1967) in Appendix II figure 2.

These data show that our results, obtained by averaging gravimetric and atomic absorption values, for two separate openings differ from the reported interlaboratory mean by 0.01 percent and 0.04 percent, respectively, and from one another by 0.05 percent. Since these values are smaller than those directly associated with K concentration determinations discussed above, they are ignored for the purposes of estimating errors.

The above treatment of errors in potassium concentrations does not consider the involvement of any judgment or experience in the data acquisition process. The treatment assumes that each data point is just as

reliable as any other, while experience may indicate much more confidence in some results than in others. In this study all the data obtained are presented in the figures described above. No data were rejected and no analysis was repeated.
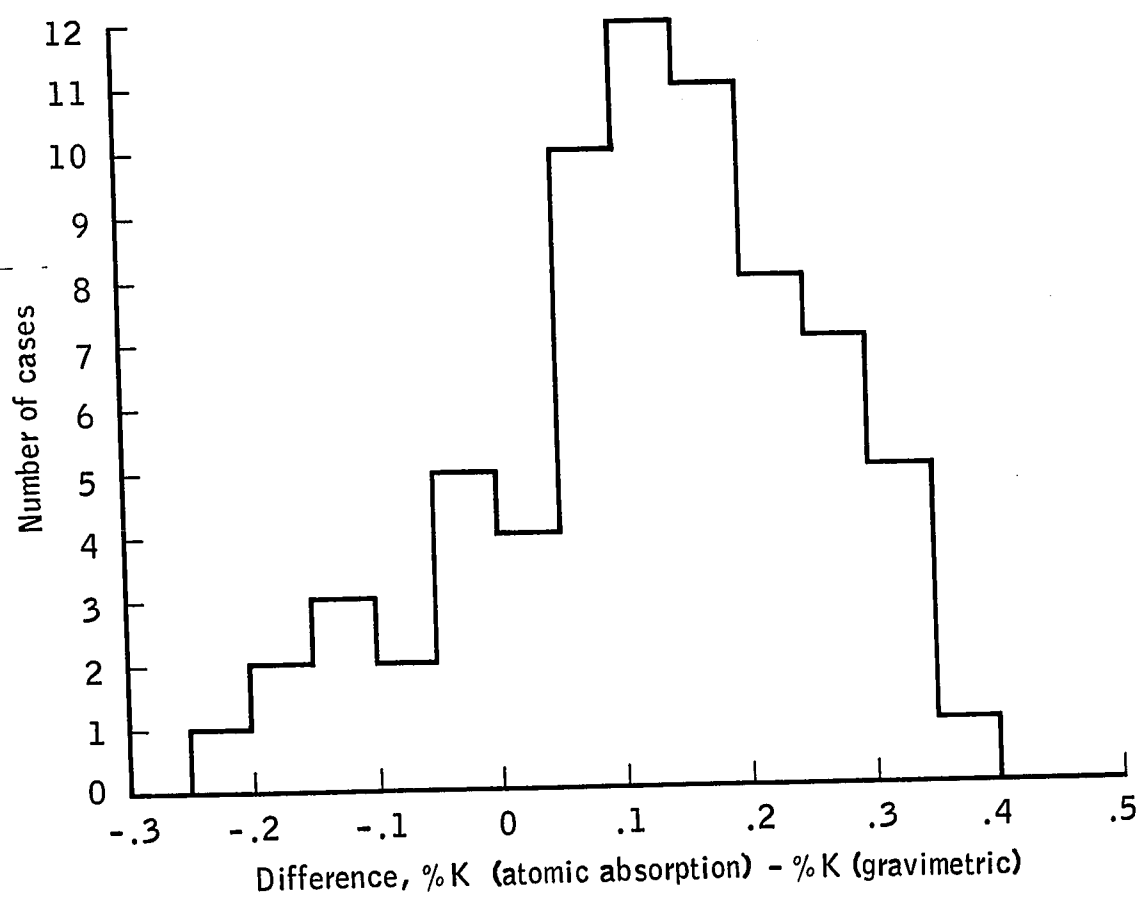
Appendix II - figure 1.- Frequency distribution of differences of potassium concentrations determined using atomic absorption and gravimetric methods.

Results of analyses by the author

from Lanphere and Dalrymple (1967)

Mean = 8.54%
Median = 8.59%
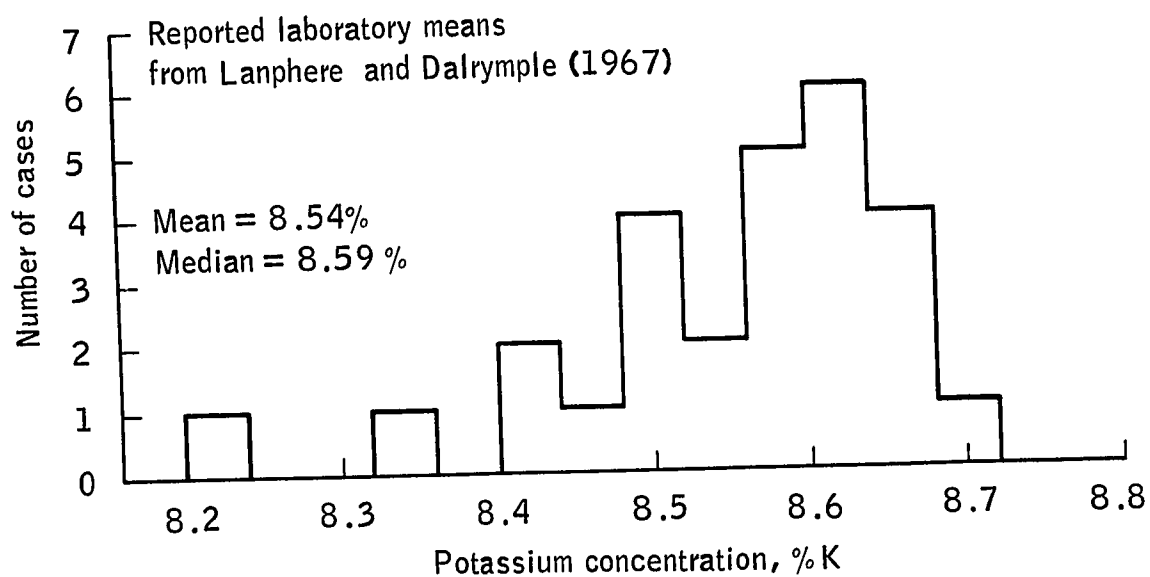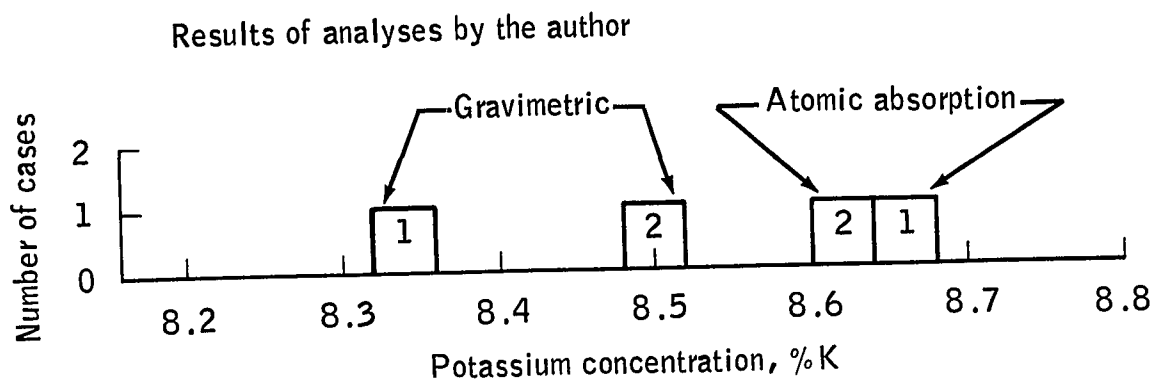
Appendix II - figure 2. - Frequency distribution of potassium concentrations reported for the U.S.G.S. Standard Muscovite, P-207.

APPENDIX III - RADIOGENIC ARGON-40 CONCENTRATION DETERMINATION

Radiogenic Ar^{40} was determined by isotope dilution mass spectrometry. In this method, a known quantity of argon spike of known isotopic composition, but principally Ar^{38}, is thoroughly mixed with gases released during fusion of the sample. Since the isotopic composition of any atmospheric argon contamination is known, the absolute quantity of radiogenic Ar^{40} may be determined. The calculations for this are presented in Appendix IV.

Instrumentation. - The mass spectrometer used was originally designed and constructed at the Humble Oil and Refining Company Houston Research Center (now Esso Production Research Company). Subsequently, the instrument was substantially rebuilt at Rice University. The instrument utilizes inflection-point focusing, which was developed by Kerwin (1949) and Hintenberger (1949). The sensitivity of the instrument is such that a signal of 8.3 millivolts is developed across a 5 x 10^{10} ohm resistor when 10^{-12} moles of argon gas is in the mass spectrometer. The instrument is operated in the static mode and has resolution of one in 125 mass units. The mass spectrometer equipment consists of the following components.

1. The gas handling system is designed to remove as much of the non-argon gaseous material released by fusion of the sample as possible. The gas clean-up is accomplished by cold trapping at liquid nitrogen temperatures and titanium foil gettering. A schematic drawing of the gas handling system is shown in Appendix III figure 1.

2. The induction furnace is used to fuse the sample which is contained in a molybdenum crucible mounted in the fusion tube. The energy is provided by a Lepel 2.5 kilowatt R. F. generator.

3. The vacuum system consists of a Vacsorb molecular sieve roughing pump, four Varian 8 liter/sec ion pumps and a Varian 50 liter/sec titanium sublimation pump. Their positions relative to the gas handling system are indicated on the schematic in Appendix III figure 1.

4. The analyzer tube and mounting were fabricated from type 304 stainless steel. The tube was bent 38.7 degrees as required by the inflection-point focusing design. The radius of curvature of this section was 8.5 inches.

5. The ion source creates a stream of argon ions by bombardment of argon atoms with electrons to form argon ions, which are then accelerated down an electric potential gradient. Electrical characteristics of the ion source are similar to those of the source used by Nier (1947).

6. The magnet is an electromagnet salvaged from a commercial spectrometer which had a conventional 60 degree sector, 6-inch radius analyzer tube. The magnet produces a field of 2000 gauss using a current of 200 milliamps at 3000 volts.

7. The ion collector assembly consists of a suppressor plate, three ion collector plates, and a housing. Quartz spacers provide electrical insulation. Ions of a single mass-to-charge ratio enter the collector through a single 0.035-inch wide slit in the suppressor plate. Three slits may be used with the three collector plates if it is desired.

8. The electronics include a high voltage supply and voltage divider used for the ion source, the filament emission regulator, and the magnet power supply. The signal voltage developed by the

ion currents flowing through a 5 x 10^{10} ohm load resistor is measured by an Applied Physics Laboratory vibrating reed electrometer system and is recorded by a Minneapolis Honeywell-Brown recorder.

Step-by-step procedures. - The detailed step-by-step procedures used at the Rice University geochronology laboratory for argon isotopic analysis is presented below.

1. Load sample.

   - Valves connecting fusion section with spike system, titanium furnace, and pump should be closed.

   - Remove fusion tube from fusion section.

   - Wash fusion tube with water.

   - Fill fusion tube about half full with 1:1 HNO_3, and leave it for about 10 minutes.

   - Remove molybdenum crucible from hook, and weigh it empty, being careful to avoid touching the crucible.

   - Add sample to crucible and weigh again.

   - Record weight of sample.

   - Return crucible to hook.

   - Pour 1:1 HNO_3 from fusion tube and rinse the tube with water.

   - Scrub fusion tube with soap and water and rinse with water.

   - Fill fusion tube about half full of 1:1 HNO_3 again and leave for about 10 minutes.

   - Pour out 1:1 HNO_3 and rinse tube with water.

   - Thoroughly rinse fusion tube with acetone.

   - Dry fusion tube with heat gun.

- Place copper gasket at mouth of fusion tube, being careful to avoid touching gasket or inside of tube.

- Replace fusion tube on fusion section so that crucible hangs without touching sides of tube and firmly tighten six nuts. No chlorinated hydrocarbons or hydrochloric acid should be used in contact with interior vacuum parts because of the danger of forming H^1Cl^{37} ions that are indistinguishable from the ions of the Ar^{38} isotopic spike.

2. Obtain vacuum.

- Install container around Vacsorb pump.

- Fill container with liquid nitrogen and continue to fill container until vigorous boiling stops.

- Check position of isolation hand valves and turn off the power supply to the appropriate ion pump(s) and titanium sublimation pump, if necessary.

- Close titanium sublimation pump hand valve, and open Vacsorb hand valve and fusion section hand valve(s), if necessary.

- Open fusion section - pump valve. Open slowly to avoid blowing sample out of crucible. Note: All metal valves are opened by taking 2 1/2 turns counter clockwise.

- Heat fusion section with heat gun 15-20 minutes.

- Keep Vacsorb pump container filled with liquid nitrogen.

- Wait 10-20 minutes to allow fusion section to cool and Vacsorb to pump.

- Turn power supply for ion pump(s) on with the scale select switch at "4kv." If half scale is reached, ion pump(s) are probably on.

- Close Vacsorb hand valve.

- Turn titanium sublimation pump on to 100 percent at first. After about 10 minutes, or as appropriate, the titanium sublimation pump may be set to operate from 0 to 5 minutes out of every 5 to 65 minutes.

- Remove Vacsorb pump container and pour remaining liquid nitrogen into a dewar.

- When the pressure at the ion pump reaches 10^{-5}mm of Hg, open the fusion section - titanium furnace valve. Pressures are determined by reading current from the ion pump power supply dial and reading the current vs. pressure chart to obtain the pressure.

- Set titanium furnace variac to 90.

- Continue to pump until pressure indicated at ion pump is below 5×10^{-7} mm of Hg. This step may take from 10 to 30 hours.

- Close fusion section - titanium furnace valve, and observe indicated pressure drop. Note: Metal hex-head valves should be closed with a torque of 30 ft-lb.

- If indicated pressure is less than 2×10^{-7} mm Hg, continue to the next section. If not, open fusion section - titanium furnace valve and wait a while longer.

3. <u>Spike introduction.</u>

- If east and west systems are not isolated, also close opposite fusion section - titanium furnace valve.

- Open spike inlet valve, and observe pressure surge as remainder of previous spike is pumped away.

- Wait until pressure stabilizes at a value near that previously indicated.

- Turn glass metering stopcock 180° clockwise to "fill" position. Special precautions must be taken not to break this valve or force the stopcock grease out.

- Open spike reservoir glass valve by turning 90° counterclockwise.

- Wait 10 minutes.

- Close spike reservoir glass valve by turning 90° clockwise.

- Close fusion section - pump valve.

- Turn metering stopcock 180° clockwise to "dump" position.

- Begin sample fusion procedure, and wait 25 minutes.

4. <u>Sample fusion.</u>

- Turn on induction furnace cooling water valve.

- Turn on induction furnace power supply switch at side of unit. Note: If water pressure is low, automatic cut-off switch may require manual operation to permit unit to operate. Under low water pressure conditions, overheating of the induction coil should not be allowed to go so far as to produce steam at the cooling water outlet.

- Install induction furnace coil around fusion tube so that the top coil is at the same level as the top of the crucible. The coil should not touch the fusion tube.

- After 25 minute wait, indicated above, is completed, close spike inlet valve.

- Push black "start" button on induction furnace.

- Increase plate current slowly to a maximum of 0.6 ampere by turning "power" knob. "Grid" knob should be set at about 80. Fusion of sample should not require more than 15 minutes. If condition of fusion tube permits, fusion may be observed visually. When bubbling activity in the crucible stops, fusion is considered to be completed.

- Turn "power" knob down to a setting of about 10-15.

- Push red "stop" button.

- Remove induction furnace coil from the fusion tube.

- After initiating gas clean-up procedures, turn induction furnace power supply switch off and close cooling water valve.

5. <u>Gas clean-up</u>.

- Remove resistance furnace from charcoal finger.

- Fill two dewars with liquid nitrogen. Place one around the cold trap and the other around the charcoal finger.

- Keep the dewars filled until vigorous boiling stops.

- Check to be sure titanium furnace is red hot.

- Open fusion section - titanium furnace valve.

- Remove dewars and install resistance furnace around charcoal trap. Setting of charcoal finger variac should always be 50.

- Cool titanium furnace slowly by turning the titanium furnace variac from 90 to 80, 80 to 70, 70 to 55, and 55 to 10 over the period of an hour.

6. Mass spectrometric analysis.

- Turn on 5 kV RF power supply.

- Turn magnet power supply control knob to 70.

- Turn magnet current control knob to obtain a reading of 85 ma on the magnet current control meter; then turn dial to obtain a reading of 75 ma.

- Turn up emission regulation to achieve plateau reading of 20 microamps on center dial.

- Turn electrometer scale to 10 mv.

- Turn on sweep, and set sweep rate at 5.

- Turn on chart drive.

- Close micrometer inlet valve.

- Close mass spectrometer pump valve.

- If measurement of the background in the tube is desired, turn sweep to down and allow sweep to continue to 50 ma on the magnet current control dial before proceeding to the next step.

- Open charcoal trap - mass spectrometer valve.

- Starting at a reading of about 75 ma on the magnet current control meter, turn sweep to down and immediately open the micrometer inlet valve to a setting of about 0025; then close the valve to avoid admitting too much gas to the ion source.

- The mass-40 peak should be observed at a value on the magnet current control meter of between 65 and 70 ma.

- By adjusting sweep rate and direction, the top of the mass-40 peak should be held.

- Open micrometer inlet valve slowly to a setting of about 0200 and adjust electrometer scale to keep the mass-40 peak on the chart recorder scale as the peak builds up.

- When the mass-40 peak stops increasing, the mass-40, mass-38, and mass-36 peaks may be measured by appropriate adjustment of the sweep rate and direction controls and the electrometer scale select knob.

- Upon completion of as many peak measurements as are judged necessary, sweep back to a reading of 75 ma on the magnet current control meter.

- Turn sweep to "hold."

- Turn sweep control off.

- Manually turn magnet current control knob down to zero.

- Turn magnet power supply control knob to zero.

- Turn emission regulation to zero.

- Turn 5 kV RF power supply off.

- Turn chart drive off and remove chart paper.

- Close charcoal trap - mass spectrometer valve.

- Open to setting of 0250 the micrometer inlet valve.

- Open the mass spectrometer pump valve, being careful to avoid
  a surge of gas which would shut down the ion pump.

7. <u>Record data.</u>

- Record the measured mass-40, mass-38, and mass-36 peaks in volts
  in the lab notebook.

- The following additional data should be recorded in duplicate
  in the lab notebook:

  a. Sample number

  b. Sample type

  c. Date

  d. Operator

  e. Sample weight

  f. Potassium concentration

  g. Spike number

  h. System used (east or west) and fusion section volume

- After calculating the apparent age, as described in Appendix IV,
  recording the following results in the lab notebook:

  a. Percent radiogenic argon

  b. Corrected Ar^{40}/Ar^{38} ratio

  c. Moles radiogenic Ar^{40}/gm sample

  d. Moles radiogenic Ar^{40}/gm K

  e. Apparent age

Radiogenic Ar^{40} concentration errors. - The errors entering into the radiogenic Ar^{40} concentration determination are of three types.

1. External experimentally derived constants.

   - atmospheric argon isotopic composition.

   - ideal gas constant.

2. Internal calibration measurements.

   - spike argon isotopic composition.

   - initial mole fraction of Ar^{38} in the spike reservoir.

   - initial pressure, volume, and temperature of the spike reservoir.

   - volumes of tubing in the fusion section and the spike system.

3. Analytical errors

   - sample weight measurement

   - mass-40, mass-38, and mass-36 measurements, or more correctly, the ratio of these masses.

Errors in the experimentally derived constants are assumed to be less than 0.01. The errors in the internal calibration measurements are unknown to the writer and are optimistically assumed to be less than 0.01. Of the analytical errors the sample weight measurement error is less than 0.01. The measurement of the relative abundance of argon isotopes is probably the source of the greatest error in the radiogenic Ar^{40} determination. An initial estimate of this error is made by referring to Appendix III figure 2, frequency distributions of radiogenic Ar^{40} measurements made by various laboratories and by this laboratory using the U.S.G.S. standard muscovite, P-207. The estimated probable error associated with the radiogenic Ar^{40} concentration determination, based on these data, is given by:

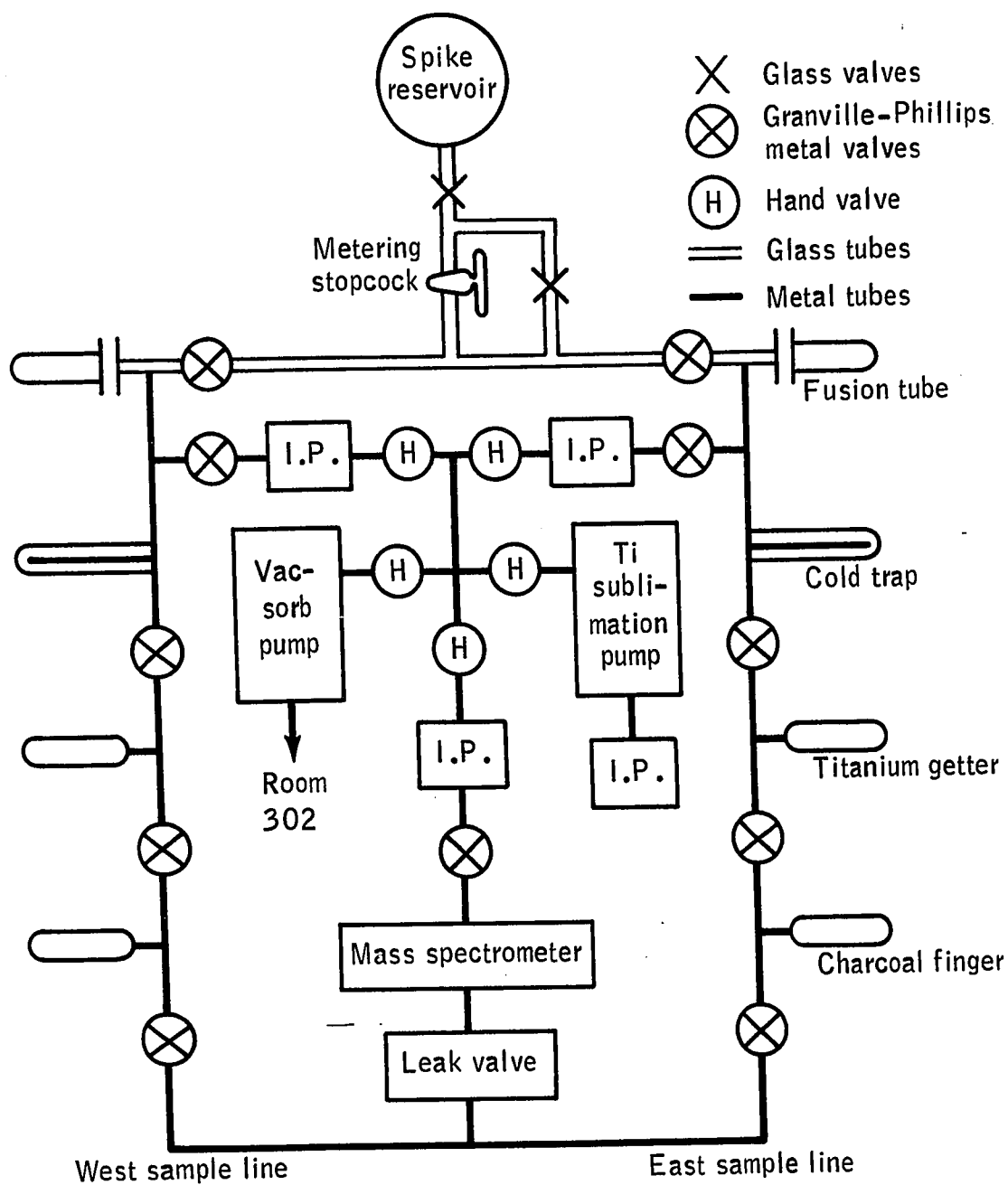$$\frac{\Delta\ Ar^{40}}{Ar^{40}} = 0.02$$

Since it is expected that this error should be higher in cases where there is a large atmospheric correction, it is suggested that the error be divided by the ratio of radiogenic to total Ar^{40} present. This is equivalent to dividing the error by the radiogenic Ar^{40} fraction, which is given by:

$$\text{Radiogenic } Ar^{40} \text{ fraction} = \frac{Ar^{40} \text{ (radiogenic)}}{Ar^{40} \text{ (atmospheric)} + Ar^{40} \text{ (radiogenic)}}$$
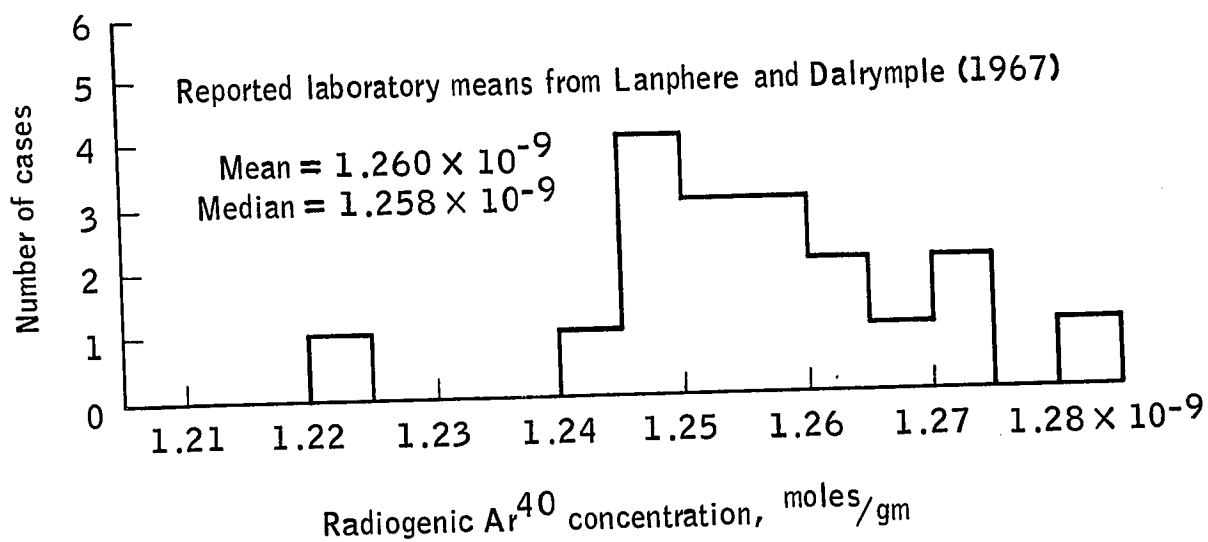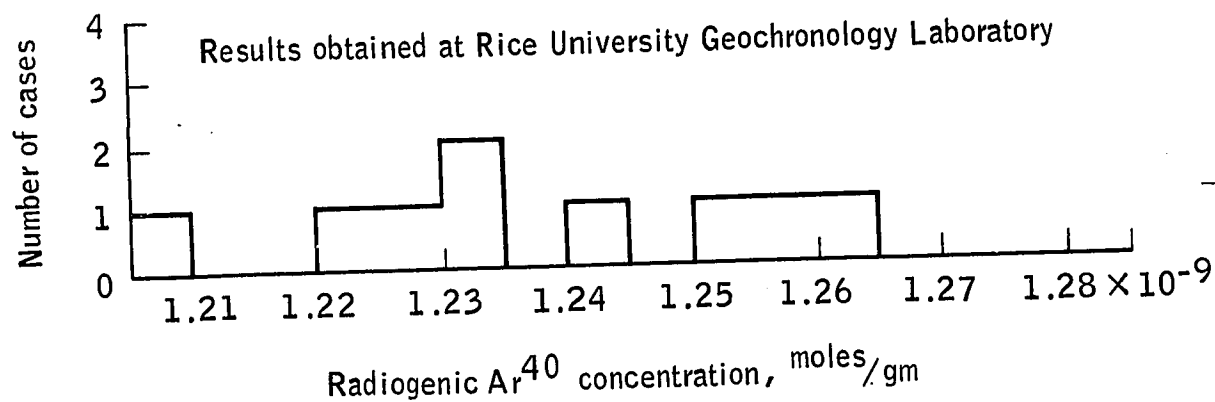
The improved estimate of the probable error for the radiogenic Ar^{40} concentration determination may then be written:

$$\frac{\Delta Ar^{40}}{Ar^{40}} = \frac{0.02}{Ar^{40} \text{(rad.) fraction}}$$

The above treatment of errors again ignores any contribution of judgement or experience in estimating the quality of a particular data point. Essentially, all the Ar^{40} data obtained were presented here. Procedural mistakes required that three argon analyses be made twice. Improved data were obtained in each case. Duplicate results were obtained for only two critical samples. The remaining samples were analyzed only once.

Spike reservoir

X Glass valves

⊗ Granville-Phillips metal valves

(H) Hand valve

Glass tubes

Metal tubes

Metering stopcock

Fusion tube

I.P. (H) (H) I.P.

Vac-sorb pump

(H) (H)

Ti sublimation pump

Cold trap

Room 302

(H)

I.P.

I.P.

Titanium getter

Mass spectrometer

Charcoal finger

Leak valve

West sample line

East sample line

Appendix III - figure 1. - Mass spectrometer gas handling system schematic.

Appendix III - figure 2. - Frequency distribution of radiogenic Ar^{40} concentrations reported for the U.S.G.S. Standard Muscovite, P-207.

APPENDIX IV - K-Ar AGE CALCULATIONS

K-Ar Age Equation. Since the decay of a particular radioactive isotope is a random process, the number of decay events per unit time interval in a given sample is directly proportional to the number of radioactive nuclides present in the sample. This relationship may be expressed as follows:

$$\frac{dN}{dt} = \lambda N$$

where N = the number of radioactive (parent) nuclides at time = t

   t = time expressed as an age, t = 0 at present and is positive toward the past.

   λ = proportionality or decay constant

Equation (1) may be written:

$$\frac{dN}{N} = \lambda dt$$

and integrated to give

$$\ln N = \lambda t + \ln P$$

where lnP is the integration constant and equivalent to the natural logarithm of the number of parent nuclides at t = 0, the present.

$$\ln N - \ln P = \ln \frac{N}{P} = \lambda t$$

taking the antilogarithm

$$\frac{N}{P} = e^{\lambda t}$$

$$P = Ne^{-\lambda t}$$

The present number of radiogenic (daughter) nuclides, D, produced in a sample of age = t is given by

$$D = N-P = N - Ne^{-\lambda t} = N(1-e^{-\lambda t})$$

Dividing by the previous equation yields

$$\frac{D}{P} = \frac{N (1 - e^{-\lambda t})}{N e^{-\lambda t}} = \frac{1 - e^{-\lambda t}}{e^{-\lambda t}} = e^{\lambda t} - 1$$
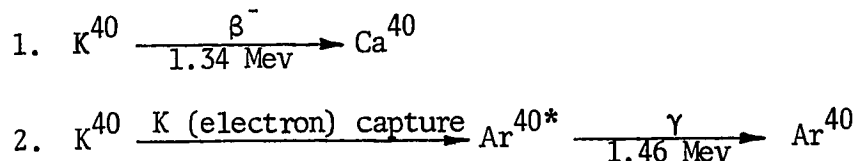
$$e^{\lambda t} = 1 + \frac{D}{P}$$

taking the natural logarithm

$$\lambda t = \ln (1 + \frac{D}{P})$$

$$t = \frac{1}{\lambda} \ln (1 + \frac{D}{P}) \qquad\qquad (2)$$

Equation (2) is the expression for the age of a sample, t, as a function of the present number of atoms or moles of the parent and daughter nuclides per unit sample weight.

The two major modes for the decay of the nuclide, K^{40}, are discussed by Houtermans (1966).

$$1. \quad K^{40} \xrightarrow[\text{1.34 Mev}]{\beta^{-}} Ca^{40}$$

$$2. \quad K^{40} \xrightarrow{\text{K (electron) capture}} Ar^{40*} \xrightarrow[\text{1.46 Mev}]{\gamma} Ar^{40}$$

The decay constants for each process are λ_β and λ_K, respectively. The constant for the decay of K^{40} is given by

$$\lambda_{K^{40}} = \lambda_\beta + \lambda_K$$

The extent to which K^{40} decays directly to the ground state of Ar^{40} without producing a 1.46 Mev γ - ray is considered negligible by Aldrich and Wetherill (1958).

The number of each daughter nuclide produced is similarly related to their respective decay constants.

$$\frac{dCa^{40}}{dt} = \lambda_\beta K^{40} \quad \text{and} \quad \frac{dAr^{40}}{dt} = \lambda_\beta K^{40}$$

where K^{40}, Ca^{40}, and Ar^{40} represent the number of atoms or moles of K^{40}, Ca^{40}, and Ar^{40} per unit sample weight.

Therefore,

$$\frac{Ca^{40}}{\lambda_\beta} = \frac{Ar^{40}}{\lambda_K} = \frac{Ca^{40} + Ar^{40}}{\lambda_\beta + \lambda_K}$$

The total number of daughter atoms or moles produced is given by

$$D = Ca^{40} + Ar^{40} = \frac{\lambda_\beta + \lambda_K}{\lambda_K} Ar^{40}$$

Thus, equation (2) modified for the decay of K^{40} becomes

$$t = \frac{1}{\lambda_\beta + \lambda_K} \ln (1 + \frac{\lambda_\beta + \lambda_K}{\lambda_K} \frac{Ar^{40}}{K^{40}}) \qquad (3)$$

The values of λ_β and λ_K used are the same as those reported by Aldrich and Wetherill (1958) and Lamphere and Dalrymple (1967).

$$\lambda_\beta = 4.72 \times 10^{-10} \text{ yr.}^{-1}$$
$$\lambda_K = 0.585 \times 10^{-10} \text{ yr.}^{-1}$$

K^{40} Equation.

Equation (3) requires a value for the total number of moles of K^{40} in a given sample. An expression for that value is presented by Lipson (1958).

$$K^{40} = \frac{(S)(\%K)/100)(K^{40}/K_{total})}{(\text{atomic wt. K})} \qquad (4)$$

where S = mass of sample, gm

%K/100 = mass fraction of K in sample

K^{40}/K_{total} = atom or mole fraction of K^{40} in natural potassium

= 0.000119 (Neir, 1950)

atomic wt. K = atomic weight of potassium = 39.1 $\frac{gm}{mole}$

The measurement of total K concentration, %K, in a sample as a weight percent is described in Appendix II.

Radiogenic Ar^{40} Equations. The results of the procedures discussed in Appendix III are values, measured in volts, of three peak heights, which correspond to mass numbers 36, 38, and 40. The mass-36 and mass-38 peaks both consist of spike and atmospheric components. The mass-40 peak consists of spike, atmospheric, and radiogenic components. Since besides the three peak heights, the spike and atmospheric isotopic compositions are known, the atom or mole ratio of radiogenic Ar^{40} to spike Ar^{38} may be calculated (Lipson, 1958).

$$(5)$$

$$\frac{Ar^{40}}{Ar^{38}(\text{spike})} = \frac{\text{mass}-40}{\text{mass}-38}\left[1 + \frac{1 - S_{38}^{36}\left(\frac{\text{mass}-38}{\text{mass}-36}\right)}{\left(\frac{\text{mass}-38}{\text{mass}-36}\right)a_{38}^{36} - 1}\right] - \frac{1 - S_{38}^{36}\left(\frac{\text{mass}-38}{\text{mass}-36}\right)}{\left(\frac{\text{mass}-38}{\text{mass}-36}\right)a_{40}^{36} - a_{40}^{38}} - S_{38}^{40}$$

where Ar^{40} = atoms or moles radiogenic Ar^{40}

Ar^{38} (spike) = atoms or moles spike Ar^{38}

mass-40 = mass-40 peak height, volts

mass-38 = mass-38 peak height, volts

mass-36 = mass-36 peak height, volts

$S_{38}^{36} = Ar^{36}/Ar^{38}$ ratio in spike = 0.000184

$S_{38}^{40} = Ar^{40}/Ar^{38}$ ratio in spike = 0.00810

$a_{38}^{36} = Ar^{36}/Ar^{38}$ ratio in atmosphere = 5.35

$a_{40}^{36} = Ar^{36}/Ar^{40}$ ratio in atmosphere = 0.00338 ⎫ (Nier, 1950)

$a_{40}^{38} = Ar^{38}/Ar^{40}$ ratio in atmosphere = 0.00064 ⎭

The number of moles of Ar^{38} in a given spike is given by:

Ar^{38} (spike) = $F_s N_s$

where N_s = the number of moles of gas in a given spike

F_s = the mole fraction of Ar^{38} in the spike = 0.783

The number of moles of gas in a given spike may be determined using the perfect gas relationship,

$$P_f V_f = N_s R T_f$$

$$N_s = \frac{P_f V_f}{R T_f}$$

Where P_f = pressure in fusion section, mm Hg

V_f = volume of fusion section, cm^3

T_f = temperature in fusion section, °K

R = ideal gas constant = $62,300 \frac{mm\ Hg\ cm^3}{mole\ °K}$

The pressure in the fusion section is a function of the number, n, of spikes removed from the reservoir and results from the expansion of gas from the metering stopcock, which may be represented as follows:

$$\frac{P_n V_m}{T_m} = \frac{P_f (V_f + V_s + V_m)}{T_f}$$

where P_n = pressure in metering valve of the nth spike removed from the spike reservoir, mm Hg

V_m = volume of metering stopcock = 0.947 cm^3

T_m = temperature in metering stopcock, °K

V_s = volume of spike system tubing between metering stopcock and fusion section = 94.0 cm^3

Assuming $T_m = T_f$

$$P_f = \frac{P_n V_m}{(V_f + V_s + V_m)} \tag{8}$$

The expression for the pressure in the metering valve, P_n, may be found by considering the following relationships:

$$\frac{P_o V_o}{T_o} = \frac{P_1 (V_m + V_o)}{T_1}$$

Subscript o refers to original conditions in spike reservoir.

Subscript 1 refers to first spike, etc.

$$P_1 = \frac{P_o V_o}{(V_m + V_o)} \frac{T_1}{T_o}$$

Since the pressure in the spike reservoir is reduced to P_1 after removal of the first spike,

$$\frac{P_1 V_o}{T_1} = \frac{P_2 (V_m + V_o)}{T_2}$$

Assuming $T_1 = T_2$

$$P_2 = \frac{P_1 V_o}{(V_m + V_o)} = \frac{P_o V_o^2}{(V_m + V_o)^2} \frac{T_1}{T_o}$$

By the same process

$$P_3 = P_o \left(\frac{V_o}{(V_m + V_o)}\right)^3 \frac{T_1}{T_o}$$

and

$$P_n = P_o \left(\frac{V_o}{(V_m + V_o)}\right)^n \frac{T_1}{T_o} \tag{9}$$

where P_o = original pressure of spike reservoir = 0.00581 mm Hg

V_o = original volume of spike reservoir = 3100. cm.^{3}

$\dfrac{T_1}{T_o}$ = ratio of temperature at first spike removal to

temperature when P_o and V_o were measured = 273./297.

Equations (6), (7), (8), and (9) may be combined to give an expression for the number of moles of Ar^{38} in the nth spike, assuming $T_1 = T_2 = T_n = T_m$.

$$Ar^{38} \text{ (spike)} = \left(\frac{F_s V_f P_o}{R \, T_o}\right) \left(\frac{V_m}{V_f + V_s + V_m}\right) \left(\frac{V_o}{V_m + V_o}\right)^n \quad (10)$$

Equation (5) may be multiplied by this result to yield the number of moles of radiogenic Ar^{40} in the sample.

Computer Program. Equations (3) through (10) have been programmed for the Olivetti-Underwood Programma 101 desk computer by Mr. G. E. Fryer. Inputs to the program are:

1. mass-40 peak, volts

2. mass-38 peak, volts

3. mass-36 peak, volts

4. sample system (W for west, Z for east)

5. n, spike number

6. S, sample mass, gm

7. %K, potassium concentration, percent

The fusion section volumes, V_f, for each sample system consist of two components, the fusion section tubing and the fusion tube itself. When

a fusion tube is replaced, its volume is determined by weighing the distilled water required to fill the tube and multiplying by the density of water, which is assumed to be 1.00 The volumes of the fusion sections are given by:

1. V_f (east) = 865. + east fusion tube volume.

2. V_f (west) = 166.4 + west fusion tube volume.

These values are stored in the D and d registers, respectively, in the program. The selection of the sample system (W or Z, above) introduces the appropriate V_f into the computation.

Outputs from the program are:

1. radiogenic Ar^{40} fraction

2. corrected Ar^{40}/Ar^{38} ratio

3. fusion section volume, V_f, used, cm^3

4. (moles radiogenic Ar^{40}/gm of sample) x 10^8

5. (moles radiogenic Ar^{40}/gm of potassium) x 10^6

6. apparent age of sample, yr. x 10^{-6}

The following constants are generated by the program.

$$\frac{K^{40}/K_{Total} \times 10^8}{(100)(atomic\ wt.\ K)} = 3.04, \frac{moles}{gm} \times 10^{-6}$$

$$\frac{P_o F_s V_m}{RT_o} \times 10^8 = 0.0232,\ moles\ \times 10^{-8}$$

$$V_m + V_s = 95.0\ cm^3$$

$$\frac{V_o}{V_o + V_m} = 0.999695$$

$$S_{38}^{36} = 0.0000184$$

$$S_{38}^{40} = 0.00810$$

$$a_{38}^{36} = 5.35$$

$$a_{40}^{36} = 0.00338$$

$$a_{40}^{38} = 0.00064$$

$$\frac{10^{-6}}{\lambda_\beta + \lambda_K} = 1885., \text{ yr. } \times 10^{6}$$

$$\frac{\lambda_\beta + \lambda_K}{\lambda_K} = 9.06$$

A list of machine language instructions for the computer program is presented in Appendix IV Table I. Indicated in the table are the general functions performed and the individual operation corresponding to each instruction. A computer printout of the program and an example computation are presented in Appendix IV figure 1 and Appendix IV figure 2, respectively.

APPENDIX IV

TABLE I

OLIVETTI UNDERWOOD PROGRAMMA 101 MACHINE LANGUAGE

FOR K-Ar AGE CALCULATION PROGRAM

Machine Language	Specific Operation	General Function
A V	Initial reference point.	Initiate program.
S	Enter (mass-40) in M Reg.	Input of mass-40, mass-38, and mass-36 data and calculation of mass-40/mass-38 and mass-38/mass-36 ratios
↓	Transfer (mass-40) to A Reg.	
S	Enter (mass-38) in M Reg.	
÷	Form (mass-40/mass-38) in B Reg.	
B ↕	Store (mass-40/mass-38) in B Reg.	
↓	Transfer (mass-38) to A Reg.	
S	Enter (mass-36) in M Reg.	
÷	Form (mass-38/mass-36) in A Reg.	
a ↑	Generate following constant in M Reg.	Compute $\dfrac{Ar^{40} \ (radiogenic)}{Ar^{38} \ (spike)}$
R ÷	4	
R ◇	8	
R ↓	1	
R S	0	
R S	0	

$+0.000184 = S^{36}_{38}$

R S   0

d S   +0.

↕   Transfer (0.00184) to A Reg. and
         (mass-38/mass-36) to M Reg.

X   Form (0.000184)(mass-38/mass-36) in A Reg.

b ↕   Store above product in b Reg.

↕   Transfer (mass-38/mass-36) to A Reg.

a ↑   Generate following constant in M Reg.

R -   5

R ↕   3 $+5.35 = a^{36}_{38}$

d -   +5.

↕   Transfer (5.35) to A Reg. and (mass-38/
         mass-36) to M Reg.

X   Form (5.35)(mass-38/mass-36) in A Reg.

C ↕   Store above product in C Reg.

↕   Transfer (mass-38/mass-36) to A Reg.

a ↕   Generate following constant in M Reg.

R ◊   8

R ↕   3

R ↕   3

R S   0 $+0.00338 = a^{36}_{40}$

R S   0

d S   +0.

X   Form (0.00338)(mass-38/mass-36) in A Reg.

a ↑   Generate following constant in M Reg.

R +   4

R X   6

R S   0

R S   0 $+0.00064 = a_{40}^{38}$

R S   0

d S   +0.

    -      Form (0.00338)(mass-38/mass-36) - (0.00064) in A Reg.

c ↕   Store above difference in c Reg.

a ↑   Generate following constant in M Reg.

d ↓   +1.

C ↓   Transfer (5.35)(mass-38/mass-36) to A Reg.

    -      Form (5.35)(mass-38/mass-36) - (1.) in A Reg

C ↕   Store above difference in C Reg.

b ↓   Transfer (0.000184)(mass-38/mass-36) to A Reg.

    ↕   Transfer above product to M Reg., and transfer (1.) to A Reg.

    -      Form (1.) - (0.000184)(mass-38/mass-36) in A Reg.

b ↕   Store above difference in b Reg.

b ↓   Transfer above difference to A Reg.

c ÷   Form $\dfrac{(1.) - (0.000184)(mass\text{-}38/mass\text{-}36)}{(0.00338)(mass\text{-}38/mass\text{-}36) - (0.00064)}$ in A Reg.

b ↓   Transfer (1.) - (0.000184)(mass-38/mass-36) to A Reg.

C ÷   Form $\dfrac{(1.) - (0.000184)(mass\text{-}38)(mass\text{-}36)}{(5.35)(mass\text{-}38/mass\text{-}36) - (1.)}$

in A Reg.

a ↑   Generate following constant in M Reg.

d ↓   +1.

+   Form $(1.) + \dfrac{(1.) - (0.000184)(mass\text{-}38/mass\text{-}36)}{(5.35)(mass\text{-}38/mass\text{-}36) - (1.)}$

in A Reg.

B X   Multiply the above by (mass-40/mass-38). Product is in A Reg.

c -   Subtract from the above product

$\dfrac{(1) - (0.000184)(mass\text{-}38/mass\text{-}36)}{(0.00338)(mass\text{-}38/mass\text{-}36) - (0.00064)}.$

Difference is in A Reg.

a ↑   Generate following constant in M Reg.

R ↓   1

R ◊   8 $+0.0081 = S^{40}_{38}$

R S   0

R S   0

R S   0

d S   +0.

-     Subtract (0.0081) from the above difference. Resulting difference is in A Reg.

B ÷   Divide above result by (mass-40/mass-38). Quotient is in A Reg.

Compute and print

$\dfrac{Ar^{40}(rad.)}{mass\text{-}40} \quad \dfrac{mass\text{-}38}{Ar^{38}(spike)}$

/	◊	Space tape once	This is considered equal to the ratio of radiogenic to total Ar^{40}.
A	◊	Print above result	

Recover and print

$$\frac{Ar^{40} \ (radiogenic)}{Ar^{38} \ (spike)}$$

This value is the corrected ratio.

B	X	Multiply above result by (mass-40/mass-38). Product is in A Reg.
B	↕	Transfer result $(Ar^{40}(rad)/Ar^{38}(spike))$ to B Reg.
B	V	Reference point for possible manual entry into the program at this point.
B	◊	Print above result.
/	◊	Space tape once

Input sample system (west or east) and spike number and print corresponding V_f.

	S	Enter sample system (W = west, Z = east). If W is entered, proceed to statement AW and continue. If Z is entered, proceed to statement AZ and continue.
A	W	Reference point for spike system subroutine.
d	↓	Transfer quantity stored in d Reg., V_f(west), to A Reg.
R	V	Transfer control of program to statement FV.
A	Z	Reference point for spike system subroutine.
D	↓	Transfer quantity stored in D Reg., V_f(east) to A Reg.
F	V	Reference point for above unconditional jump.
	S	Enter spike number, N.
A	◊	Print (V_f) selected.

D	*	Clear D Reg.
d	*	Clear d Reg.
/	◊	Space tape once.

	V	Return to starting point.	End of Part I of program

A	V	Reference point. To start part II of program push V.	Initiate Part II of program.

C	↑	Store (n) in C Reg.	Compute Ar^{38} (spike). See equation (10) of Appendix IV.
b	↕	Store (V_f) in b Reg.	
a	↑	Generate the following constant in M Reg.	

R	-	5
R	*	9
R	X	6
R	*	9
R	*	9
R	*	9
d	S	+0.

$$+0.999695 = \frac{V_o}{V_o + V_m}$$

	↓	Transfer (0.999695) to A Reg.

a	↑	b^n Subroutine used to calculate (0.999695)^n in c Reg. Initially n must be in C Reg. and (0.999695) in A Reg. See Subroutine no. 32
d	↓	

c	↑
B	V
C	↕
a	↑
R	-
d	S
	X
/	↕
	-
/	V
	↕
B	W
/	W
	Z
a	V
	↕
c	↕
C	X
c	↕
C	W
a	W
C	↕
A	X
C	V
A	Z

in "Mathematical Programming on the Programma 101." Appendix A, Math Utility Subroutines.

c $\downarrow$ Transfer $(0.999695)^n$ to A Reg.

a $\uparrow$ Generate following constant in M Reg.

R $\uparrow$ 2

R $\updownarrow$ 3

R $\uparrow$ 2

R S   0

d S   +0.

$$+0.0232 = \frac{P_o F_s V_m}{RT_o} \times 10^8,$$

$$\text{moles} \times 10^{-8}$$

X   Form $(0.0232)(0.999695)^n$ in A Reg.

b X   Multiply above product by (V_f). Product in A Reg.

c $\updownarrow$ Store above product in c Reg.

a $\uparrow$ Generate following constant in M Reg.

r -   5.

D *   +9

$$+95. = V_m \times V_x, \text{ cm}^3$$

b $\downarrow$ Transfer V_f to A Reg.

+   Form $V_f + 95.$ in A Reg.

$\updownarrow$ Transfer $V_f + 95.$ to M Reg.

c $\downarrow$ Transfer $(0.0232)(0.999695)^n V_f$ to A Reg.

$\div$ Divide above product by $V_f + 95.$ Quotient is in A Reg.

B X   Multiply above quotient by Ar^{40} (radiogenic)/Ar^{38} (spike). Product is in A Reg.

Calculate Ar^{40}(radiogenic) in units of moles $\times 10^{-8}$.

S		Enter Sample mass (S) in grams in M Reg.
÷		Divide (s) into Ar^{40}(radiogenic). Quotient is in A Reg.
A ◊		Print above quotient, (Moles Ar^{40}(radiogenic)/gm. of sample) x 10^{-8}

Input sample mass in grams and compute and print radiogenic Ar^{40} content per unit sample mass in units of (moles/gm) x 10^{-8}

S		Enter potassium concentration in percent (%K) in M Reg.
÷		Divide above value into preceding quotient. Quotient is in A Reg.
A ◊		Print resulting quotient. (Moles Ar^{40}(radiogenic)/gm of potassium) x 10^{-6}

Input potassium concentration in percent and compute radiogenic Ar^{40} content per unit mass of potassium in units of (moles/gm) x 10^{-6}

a ↑		Generate following constant in M Reg.
R +	4	
R S	0	
d ↕	+3.	
÷		Divide (3.04) into above quotient. Resulting is in A Reg.

$$+3.04 = \frac{(K^{40}/K_{Total}) \times 10^8}{(100)(at.\ wt.\ K)}, $$

moles/gm x 10^{-6}

Compute the mole ratio
$$\frac{Ar^{40}\ (radiogenic)}{K^{40}}$$

a ↑		Generate following constant in M Reg.
R X	6	

Compute and print age, t, in units of yr. x 10^6.

R	S	0	
d	*	+9.	

$$+9.06 = \frac{\lambda_\beta + \lambda_K}{\lambda_K}$$

	X	Multiply above quotient by (9.06). Product is in Reg. A.
a	↑	Generate following constant in M Reg.
d	↓	+1.
	+	Add (1.) to above product. Sum is in A Reg.
B	↕	Store above sum in B Reg.

B	↓
A	÷
	↕
	-
B	↕
	+
	↕
B	↕
	÷
A	X
c	↕
b	*
a	Z
	↓
b	↕
b	+
b	↕

Compute natural logarithm of the above sum using the ln(x) subroutine and leave the result in the A Reg. See subroutine number 1 in "Mathematical Programming on the Programma 101," Appendix A, Math Utility Subroutines.

```
B  X
c  X
B  ↕
A  ÷
   ↕
   +
   +
B  ↕
B  ÷
   ↕
   ↓
/  Z
A  ↕
/  Z
b  ↓
A  +
```

a ↑   Generate following constant in M Reg.

```
r  -        5.
R  ◊        8
R  ◊        8
d  ↓        1
```

$$+1885. = \frac{10^{-6}}{\lambda_\beta + \lambda_K} , \quad \text{yr. x } 10^6$$

   X   Multiply (1885.) times above natural
            logarithm. Product is in A Reg.

A ◊   Print above product, t, the age in m.y.

1030•000000 □◊

334•000000 d◊

Appendix IV figure 1 - Olivetti Underwood Programma 101

Printout of K-Ar Age Calculation Program

Appendix IV figure 1 - Olivetti Underwood Programma 101

Printout of K-Ar Age Calculation Program (Continued)

programma 101 olivetti underwood programma 101 olivetti underwood programma 101 olivetti underwood programma 101 olivetti underwc

```
A V
C ↑
b ↕
a ↑
R -
R ✳
R X
R ✳
k ✳
R ✳
d S
  ↓
a ↑
d ↓
c ↑
B V
C ↕
a ↑
k -
d S
  X
/ ↕
  -
  ↕
/ V
  ↕
B W
/ W
  Z
a V
  ↕
c ↕
C X
c ↕
C W
a W
C ↕
A X
C V
A Z
c ↓
a ↑
k ↑
R ↕
R ↑
R S
o S
```

Appendix IV figure 1 - Olivetti Underwood Programma 101

Printout of K-Ar Age Calculation Program (Continued)

Appendix IV figure 1 - Olivetti Underwood Programma 101

Printout of K-Ar Age Calculation Program (Continued)

ivetti underwood programma 101 olivetti underwood progra

```
a Z
  ↓
b ↕
b ✦
b ↕
B X
c X
B ↕
A ✦
  ↕
  ✦
  ✦
B ↕
R ✦
  ↕
  ↓
/ Z
A ↕
/ Z
b ↓
A ✦
a ↑
r –
R ◊
R ◊
D ↓
  X
A ◊
```

Appendix IV figure 1 - Olivetti Underwood Programma 101

Printout of K-Ar Age Calculation Program (Continued)

Olivetti underwood programma 101 olivetti underw

```
                   V
      4 • 56       S
        3 • 21     S
  0 • 0 0 3 4 5    S

  0 • 8 0 8 9 0 7  A 0
  1 • 1 4 9 1 0 0  B 0

                   W
        8 0 0      S
3 3 4 • 0 0 0 0 0  A 0

                   V
    0 • 3 4 5 6    S
  0 • 0 4 7 0 3 7  A 0
      1 • 2 3      S
  0 • 0 3 8 2 4 1  A 0
2 0 3 • 4 3 6 7 4 0  A 0
```

	Input			Output
V	Initiate program, part I		A	Radiogenic Ar^{40} fraction
S	Mass-40 peak, volts		B	Corrected ratio, $[Ar^{40}(rad.)/Ar^{38}(spike)]$
S	Mass-38 peak, volts			
S	Mass-36 peak, volts		A	Fusion section volume, V_f, cm^3
W	Sample system		A	Moles $Ar^{40}(rad.)/gm$ sample x 10^8
S	Spike number		A	Moles $Ar^{40}(rad.)/gm$ K x 10^6
V	Initiate program, part II		A	K-Ar age, m. y.
S	Sample mass, S, gm			
S	K concentration, %K			

Appendix IV figure 2 - Input-Output Format for

Olivetti Underwood Programma 101 K-Ar Age Calculation Program

APPENDIX V - ERROR ANALYSIS

The expression for the K-Ar age of a sample, as developed in the previous section is:

$$t = \frac{1}{\lambda_K + \lambda_\beta} \ln \left(1 + \frac{\lambda_K + \lambda_\beta}{\lambda_K} \frac{Ar^{40}}{K^{40}} \right) \tag{1}$$

where t = time since crystallization or age of sample

λ_K = decay constant for electron capture process, $yr.^{-1}$

λ_β = decay constant for beta decay process, $yr.^{-1}$

Ar^{40} = radiogenic Ar^{40} concentration, $\frac{moles}{gm}$

$K^{40} = K^{40}$ concentration, $\frac{moles}{gm}$

According to Scarborough (1962, p. 505), if the probable error of each element of equation (1) is known, then the probable error associated with the age of the sample, t, may be calculated by the equation,

$$\frac{\Delta t}{t} = \left[\left(\frac{\partial t}{\partial \lambda_K} \right)^2 \left(\frac{\Delta \lambda_K}{t} \right)^2 + \left(\frac{\partial t}{\partial \lambda_\beta} \right)^2 \left(\frac{\Delta \lambda_\beta}{t} \right)^2 + \left(\frac{\partial t}{\partial Ar^{40}} \right)^2 \left(\frac{\Delta Ar^{40}}{t} \right)^2 + \left(\frac{\partial t}{\partial K^{40}} \right)^2 \left(\frac{K^{40}}{t} \right)^2 \right]^{1/2}$$

It should be understood that the above equation is simplified since each element considered is in turn a function of various other independent elements. To be strictly correct a separate term should appear in the above equation for each independent parameter contributing to the age equation for which there is an associated error.

K^{40} concentration is given by equation (4) of Appendix IV and is dependent on the measured K concentration, %K. This is the only factor

in equation (4) with a probable error exceeding 0.01. The probable

error for the K concentration determination, as indicated in Appendix II,

is given by:

$$P.\ E.\ (K\ conc.) = \frac{0.1\%}{\%K}$$

and ignoring the smaller errors,

$$\frac{\Delta\%K}{\%K} = \frac{0.1}{\%K} = \frac{\Delta K^{40}}{K^{40}} \tag{3}$$

Ar^{40} concentration is a function of all the factors of equations (5)

and (10) in Appendix IV. The errors associated with each of these factors

is assumed to be either less than 0.01 or included in the estimated prob-

able error for Ar^{40} determinations given in Appendix III,

$$\frac{\Delta Ar^{40}}{Ar^{40}} = 0.02\ Ar^{40}\ (rad.)\ fraction \tag{4}$$

The decay constant values are based on counting experiments and are

given by the expressions,

$$\lambda_\beta = \frac{1}{N}\left(\frac{dN}{dt}\right)_\beta \qquad \lambda_K = \frac{1}{N}\left(\frac{dN}{dt}\right)_\gamma$$

where

$$N = \frac{(A.N.)}{(A.W.K.)}\left(\frac{K^{40}}{K\ total}\right)$$

$$(A.N.) = Avogadros\ No. = 6.02\ x\ 10^{23}\ \frac{atoms}{mole}$$

(A.W.K.) = Atomic Wt. for K = 39.1 $\frac{gm}{mole}$

$$\left(\frac{K^{40}}{K\ total}\right) = \text{constant ratio of } K^{40} \text{ to total } K = 0.000119$$

$$\left(\frac{dN}{dt}\right)_\beta = \beta \text{ decay rate, } gm.^{-1} yr.^{-1}$$

$$\left(\frac{dN}{dt}\right)_\gamma = \text{electron capture rate, } gm.^{-1} yr.^{-1}$$

(assuming that this is equal to γ emission rate)

The estimated probable errors associated with these counting rates, and the corresponding decay constants, based on data summarized by Houtermans (1966), are as follows.

$$\frac{\Delta\left(\frac{dN}{dt}\right)_\beta}{\left(\frac{dN}{dt}\right)_\beta} = 0.025 = \frac{\Delta\lambda_\beta}{\lambda_\beta} \tag{5}$$

$$\frac{\Delta\left(\frac{dN}{dt}\right)_\gamma}{\left(\frac{dN}{dt}\right)_\gamma} = 0.04 = \frac{\Delta\lambda_K}{\lambda_K} \tag{6}$$

The error factor curves for λ_β and λ_K in Appendix V figure 1 were taken from Aldrich and Wetherill (1958). The curve for Ar^{40} and K^{40} were added by the author. Each term in equation (2) may be obtained by multiplying the value given by the curve for the known age of the sample by the corresponding probable error value given in equations (3) through (6),

then squaring the result. For example, consider a sample 1000 m.y. old with 5% K concentration and a radiogenic argon fraction of 0.6.

For the λ_β term,

$$- \left(\frac{\lambda_\beta}{t} \quad \frac{\partial t}{\partial \lambda_\beta}\right)\left(\frac{\Delta\lambda_\beta}{\lambda\beta}\right) = \quad - (0.2)(0.025) = - (0.005)$$

For the λ_K term,

$$-\left(\frac{\lambda_K}{t} \quad \frac{\partial t}{\partial \lambda_K}\right)\left(\frac{\Delta\lambda K}{\lambda_K}\right) = \quad - (0.8)(0.04) = - (0.032)$$

For the Ar^{40} term,

$$\left(\frac{Ar^{40}}{t} \quad \frac{\partial t}{\partial Ar^{40}}\right)\left(\frac{Ar^{40}}{Ar^{40}}\right) = (0.78) \left(\frac{0.02}{0.6}\right) = (0.026)$$

For the K^{40} term,

$$-\left(\frac{K^{40}}{t} \quad \frac{\partial t}{\partial K^{40}}\right)\left(\frac{\Delta K^{40}}{K^{40}}\right) = -(0.78) \left(\frac{0.1}{5.0}\right) = - (0.016)$$

From Equation (2)

$$\frac{\Delta t}{t} = \left[(-0.005)^2 + (-0.032)^2 + (0.026)^2 + (-0.016)^2\right]^{\frac{1}{2}}$$

$$= 0.044$$

The probable error associated with the age of

1000 m.y. is ± 44 m.y.

The errors listed in Tables I and II were determined in the manner described here. It should be noted that a large part of the error, up to about one-half, is due to poorly known constants. This portion of the error contributes to the uncertainty of the absolute age reported, but it does not contribute to the error in the differences between two or more ages determined using the same constants. Thus, ages determined in a given study may be compared with greater confidence than the absolute value of the age of the sample may be stated.

In this analysis the error associated with the experimentally determined constant, $K^{40}/K_{total} = 0.000119$, (Neir, 1950) was not considered because the reported error was only 1%, that is,

$$\frac{\Delta \; K^{40}/K_{total}}{K^{40}/K_{total}} = 0.01$$

However, by referring to the equations for λ_β, and λ_K, and K^{40}, it may be seen that (K^{40}/K_{total}) is a common factor to them all. The error in the age of young rocks produced by an error in (K^{40}/K_{total}) will be greater than 1%. It is noted that the measurement of (K^{40}/K_{total}) has been made very few times, and that measurements of K^{39}/K^{41} have produced some variability (Letolle, 1966). The relative error in the age due to the (K^{40}/K_{total}) factor is greater than the relative error

for the value of (K^{40}/K_{total}) itself. In future error analyses more attention should be given to contribution of the (K^{40}/K_{total}) term to the error for the K-Ar age.
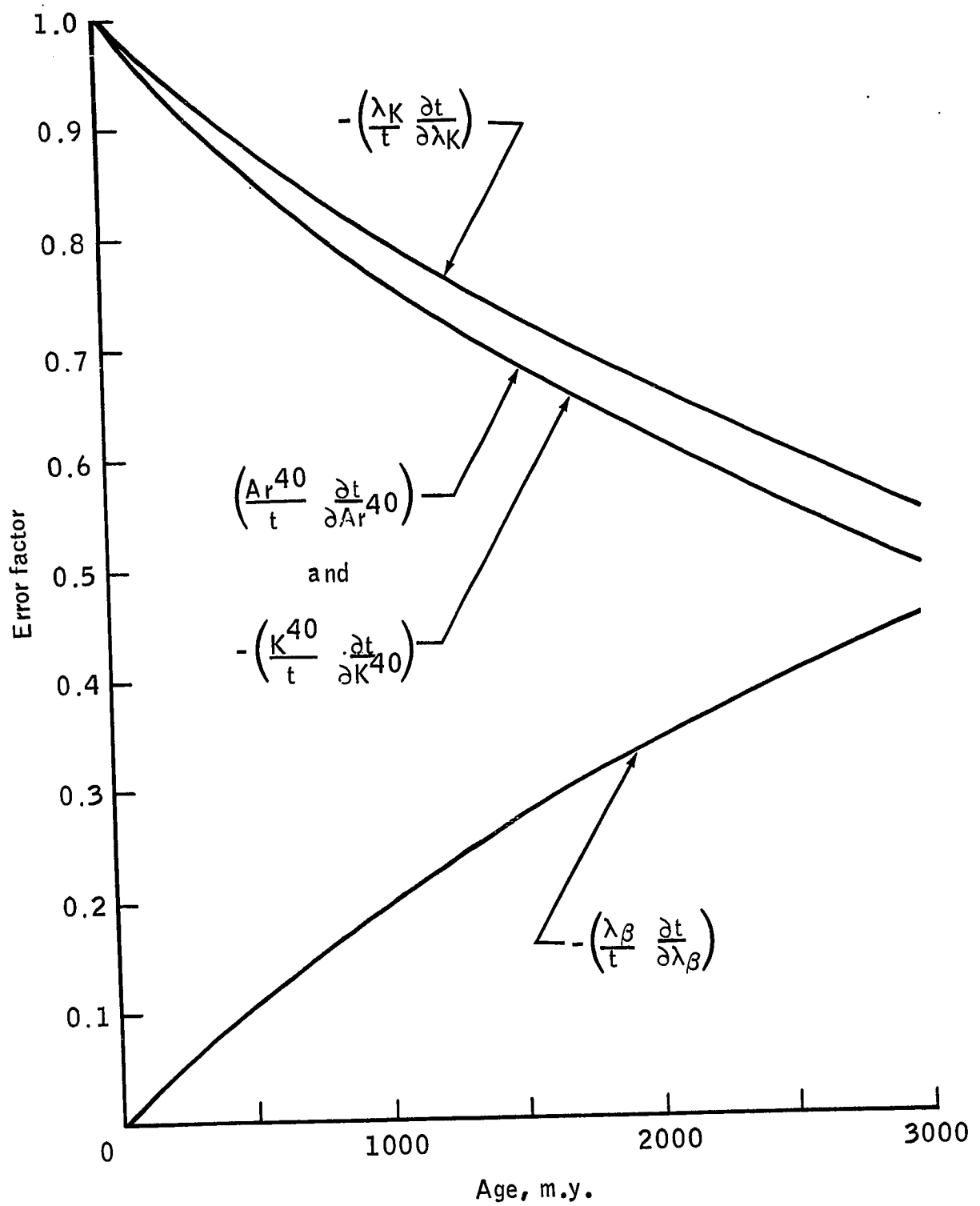
Appendix Ⅴ - figure 1. Error factor vs. age for K-Ar error analysis.